

Implications of TeV Flavor Physics for the $\Delta I = \frac{1}{2}$ Rule and $\text{BR}_\ell(B)$ ¹

Alexander L. Kagan²

Stanford Linear Accelerator Center

Stanford University, Stanford, California 94309

ABSTRACT

Two of the outstanding discrepancies between weak interaction phenomenology and the standard model come in the large size of the $\Delta I = \frac{1}{2}$ enhancement in K decays and in the small value of the B semileptonic branching ratio. We argue that these discrepancies are naturally explained by chromomagnetic dipole operators arising from new physics at the TeV scale. These operators are closely connected to diagrams which contribute to the quark mass matrix, and we show how the proper enhancement of the hadronic decays of s and b quarks can be linked to generation of particular Cabibbo-Kobayashi-Maskawa mixing angles or quark masses. We confirm our model-independent analysis with detailed consideration of supersymmetric models and technicolor models with techniscalars. This picture has additional phenomenological predictions for the B system: The branching ratio of charmless nonleptonic B decays should be of order 20%, due to a large rate for $b \rightarrow sg$, while there are no dangerous new contributions to $b \rightarrow s\gamma$. Sizable contributions to $b \rightarrow d\gamma$ are a common feature of models incorporating this mechanism. In techniscalar models the $Zb\bar{b}$ coupling is enhanced, in association with sizable contributions to $b \rightarrow s\mu^+\mu^-$.

¹Work supported by the Department of Energy, contract DE-AC03-76SF00515.

²Email: kagan@slac.stanford.edu, Address after Sep. 1: Department of Physics, University of Cincinnati.

1. Introduction

The $\Delta I = \frac{1}{2}$ rule in $K \rightarrow \pi\pi$ decays is one of the historical puzzles of particle physics. The S-wave two pion final state has total isospin 0 or 2 and one has to understand why the $\Delta I = \frac{1}{2}$ transition amplitude is larger by a factor of twenty than the $\Delta I = \frac{3}{2}$ transition amplitude. In the standard model a large non-perturbative QCD matrix-element enhancement is required. Indeed, calculations of the $\Delta I = \frac{1}{2}$ amplitude employing the $\frac{1}{N_c}$ expansion and other models of strong interaction behaviour at low energies give substantial enhancement [1, 2, 3]. Nevertheless, these estimates remain about a factor of two too small after perturbative QCD corrections at next-to-leading order are taken into account [3]. In ref. [4] a phenomenological approach suggested that important contributions could come from effective diquark states. Final state interactions might also enhance the $\Delta I = \frac{1}{2}$ amplitude and suppress the $\Delta I = \frac{3}{2}$ amplitude [5]. But neither approach is completely persuasive. Twenty years after the birth of QCD, the large size of the $\Delta I = \frac{1}{2}$ amplitude remains an important puzzle.

In the B system there is also persistent evidence for discrepancy between existing measurements and the standard model, in the semileptonic branching ratio of B 's. The world average [6] for B mesons produced at the $\Upsilon(4S)$ resonance is

$$\text{BR}_\ell(B) = 10.29 \pm .06 \pm .27\%, \quad (1)$$

and for B mesons produced at the Z resonance it is

$$\text{BR}_\ell(B) = 11.33 \pm .22 \pm .41. \quad (2)$$

On the other hand, the parton model tends to give [7] $\text{BR}_\ell(B) \gtrsim 13\%$, including leading [8, 9] and next-to-leading [10, 11] order QCD enhancement of the hadronic B meson decay width. Again, one can appeal to non-perturbative effects to resolve the discrepancy. However, a recent analysis [12] employing heavy quark effective field theory (HQET) techniques gave estimates of these non-perturbative terms which are much smaller than would be necessary. (This is still controversial [13] and is sure to be debated further in the future.)

A possibly related anomaly may be present in measurements of the charm multiplicity, n_c , in B decays. Defined as the number of charm states per B decay, one obtains $n_c \approx 1.2$ in the parton model. This exceeds 1 because of the decay channel

$b \rightarrow c\bar{c}s$. Measured values have persistently exhibited a ‘charm deficit’. Although the world average [14]

$$n_c = 1.08 \pm .06 \tag{3}$$

has recently increased, it remains consistent with a possible charm deficit. This suggests that non-charm hadronic decay channels are somehow enhanced, thus simultaneously suppressing $\text{BR}_\ell(B)$.

Perhaps the data, together with improved calculations of hadronic flavor-changing processes, is starting to tell us something about a possible role for new flavor physics. For example, it may turn out that the standard model $\Delta I = \frac{1}{2}$ enhancement, while very large, only accounts for 50% to 70% of the observed $\Delta I = \frac{1}{2}$ amplitude. A significant portion of the $\Delta I = \frac{1}{2}$ rule would still have to be accounted for in this case. It would be wonderful if the same mechanism could give an additional, exotic, channel for hadronic B decays.

In this paper, I suggest the hypothesis that there are new perturbative contributions to K and B decay amplitudes resulting from chromomagnetic dipole operators induced at TeV energies. These effects occur in a wide variety of models with new interactions at the TeV scale. For example, quark dipole moments are typical in compositeness and extended technicolor scenarios. In general, these new interactions are closely connected to diagrams which contribute to the quark mass matrix. In particular, removal of the gluon from a chromomagnetic dipole graph often leaves a finite quark mass contribution. Thus, $\text{BR}_\ell(B)$ suppression and substantial contributions to the $\Delta I = \frac{1}{2}$ amplitude might be the byproducts of new *flavor physics* which also explains features of the quark mass spectrum. We will provide model-independent arguments as well as explicit examples which demonstrate that such a connection is possible and, perhaps, even likely.

Some of the earliest suggestions for the origin of the $\Delta I = \frac{1}{2}$ rule [15, 16, 17, 18] involved new interactions which induce the $\Delta I = \frac{1}{2}$ chromomagnetic dipole operators

$$Q_G^{ds\pm} = g_s \bar{d} \sigma_{\mu\nu} t^a \frac{1 \pm \gamma_5}{2} s G_a^{\mu\nu} \tag{4}$$

via penguin graphs. In the standard model these operators are suppressed by light quark masses and their contribution to the $\Delta I = \frac{1}{2}$ amplitude is more than an order of magnitude smaller than the conventional four-fermion operator contributions. However, the requisite fermion chirality flip associated with dipole operators can be much

larger if these operators are induced by new physics; examples of this have been presented from time to time in the literature. In [15, 16, 17] the $\Delta I = \frac{1}{2}$ chromomagnetic dipole operators were induced via charm-changing right-handed charged currents coupled to the W boson. Of course this possibility has long since been ruled out. In [18] these operators were discussed in the context of multi-Higgs doublet models but their contributions were suppressed by light quark masses. An E_6 inspired model was considered in [19] in which the $\Delta I = \frac{1}{2}$ chromomagnetic operators were generated via loop diagrams containing vectorlike down quarks and neutral scalars. Finally, the authors of [20], again motivated by E_6 , found that scalar diquark exchange could generate a substantial $\Delta I = \frac{1}{2}$ amplitude via the chromomagnetic dipole operators. The authors of refs. [19, 20] eventually reached negative conclusions after invoking constraints on their models from $K - \bar{K}$ mixing.

We will demonstrate here that the $\Delta I = \frac{1}{2}$ chromomagnetic dipole operators can acquire large coefficients in supersymmetric models, and in technicolor models which employ techniscalars to generate quark masses. The corresponding contributions to the ($\Delta I = \frac{1}{2}$) $K \rightarrow \pi\pi$ amplitude first arise at order p^4 in the chiral lagrangian expansion [21], and are unfortunately difficult to estimate. But they could well account for 30% – 50% of the observed amplitude, which would significantly narrow any gap between theory and experiment. We also find that for supersymmetry with ultra-light gluinos the induced $\Delta I = \frac{1}{2}$ amplitude can be larger. In all of our examples we check that the most stringent constraints on flavor-changing neutral currents are not violated. Our results are, in particular, consistent with the known small value of $\Delta m_K \equiv m(K_L) - m(K_S)$.

New physics can also induce the $\Delta B = 1$ chromomagnetic dipole operators

$$Q_G^{sb\pm} = g_s \bar{s} \sigma_{\mu\nu} t^a \frac{1 \pm \gamma_5}{2} b G_a^{\mu\nu} \quad (5)$$

$$Q_G^{db\pm} = g_s \bar{d} \sigma_{\mu\nu} t^a \frac{1 \pm \gamma_5}{2} b G_a^{\mu\nu} \quad (6)$$

with significantly larger coefficients than in the standard model. The resulting enhancement of the B meson hadronic decay width could be large enough to solve the $\text{BR}_\ell(B)$ puzzle. The operators in (5) can increase the branching ratio for $b \rightarrow sg$ to 15 – 30%, well above what is expected in the standard model. This possibility was first pointed out in [22] in the context of two-Higgs doublet models, and more recently in [12]. This type of resolution would also lead to a charm deficit in B decays which is consistent with the measured value.

It is important to check that models of $\text{BR}_\ell(B)$ suppression do not produce large unwanted contributions to $\text{BR}(b \rightarrow s\gamma)$. CLEO has recently announced a measurement of this branching ratio [23],

$$\text{BR}(B \rightarrow s\gamma) = (2.32 \pm .51 \pm .29 \pm .32) \times 10^{-4}, \quad (7)$$

which corresponds to an upper bound of 4×10^{-4} . Unfortunately, multi-Higgs doublet models of $\text{BR}_\ell(B)$ suppression are in gross conflict with this bound [24] and are thus excluded.¹ A simple model-independent criterion will be introduced which can be used to identify models of $\text{BR}_\ell(B)$ suppression which do not run into this difficulty.

We will see that in supersymmetric models and in technicolor models with techniscalars it is easy to induce large enough coefficients for the $\Delta B = 1$ chromomagnetic dipole operators to resolve the $\text{BR}_\ell(B)$ puzzle. $B - \bar{B}$ mixing constraints are not restrictive, and electric-dipole contributions to $b \rightarrow s\gamma$ are sufficiently small. In certain cases $\text{BR}(b \rightarrow d\gamma)$ is 1 to 2 orders of magnitude larger than in the standard model, lying in the range $(.1 - 1.0) \times 10^{-4}$. This has interesting implications for observation of $B \rightarrow \rho\gamma$ or $B \rightarrow \phi\gamma$ at CLEO and future B factories. The present bound [6] is

$$\text{BR}(B \rightarrow \rho\gamma) < .34 \cdot \text{BR}(B \rightarrow K^*\gamma) \quad (8)$$

at 90% CL, which leaves a large window open for new physics.

The main point of this paper is to uncover a possible connection between certain features of the quark mass spectrum and the various puzzles outlined above. Our model-independent analysis will suggest that a substantial portion of the $\Delta I = \frac{1}{2}$ amplitude is directly associated with mass contributions which account for m_s , or θ_c . The analysis also suggests that resolutions of the $\text{BR}_\ell(B)$ puzzle attributed to chromomagnetic dipole operators are directly associated with generation of m_b , with $\sim 100 \text{ MeV}$ mass contributions which account for V_{cb} (and m_s), or with smaller mass contributions which account for V_{ub} (as well as θ_c and m_d). The supersymmetry and technicolor examples will illustrate these points explicitly. Two phenomenologically distinct possibilities for a new scale of flavor physics emerge: $M \sim 1 - 2 \text{ TeV}$ (*Region I*), which can be associated with $\text{BR}_\ell(B)$ suppression, and $M \sim \frac{1}{2} \text{ TeV}$ (*Region II*), which can be associated with both $\text{BR}_\ell(B)$ suppression and $\Delta I = \frac{1}{2}$ enhancement.

We organize our discussion as follows. To further motivate the introduction of new physics we begin in Section 2 with a review of the status of the $\Delta I = \frac{1}{2}$ rule and

¹The possibility of dangerously large contributions, in general, in multi-Higgs doublet models has been discussed in refs. [25, 26].

inclusive B decays in the standard model. A model-independent discussion of the phenomenology of chromomagnetic and electric-dipole operators and associated quark mass contributions follows in Section 3. Supersymmetry and technicolor examples are discussed in Sections 4 and 5, respectively. A discussion and summary of our results is given in Section 6. Appendix A provides further details on the relationship between the dipole operators and the quark mass spectrum, and Appendix B contains expressions for new contributions to Δm_K and Δm_B in the models we consider.

2. The $\Delta I = \frac{1}{2}$ rule and $\text{BR}_\ell(B)$ in the standard model

The amplitudes for $K^0 \rightarrow \pi^+\pi^-$ and $K^0 \rightarrow \pi^0\pi^0$ can be parametrized in terms of the $\Delta I = \frac{1}{2}$ transition amplitude, A_0 , and the $\Delta I = \frac{3}{2}$ transition amplitude, A_2 , defined as

$$A_I = \langle (\pi\pi)_I | H_W | K^0 \rangle, \quad I = 0, 2. \quad (9)$$

H_W is the weak hamiltonian and the subscripts 0, 2 denote the total $\pi\pi$ isospin. Experimentally [27]

$$|A_0| = 3.3 \times 10^{-7} \text{ GeV}, \quad |A_2| = 1.5 \times 10^{-8} \text{ GeV}, \quad (10)$$

and the $\Delta I = \frac{1}{2}$ rule is manifested by the ratio $|A_0/A_2| = 22.2$.

In the standard model the bulk of the $\Delta I = \frac{1}{2}$ amplitude is almost certainly due to the 4-quark operator hamiltonian

$$H_W = C_1 Q_1 + C_2 Q_2, \quad (11)$$

where

$$\begin{aligned} Q_1 &= [\bar{s}_\alpha \gamma_\mu (1 - \gamma_5) d_\beta] [\bar{u}_\beta \gamma^\mu (1 - \gamma_5) d_\alpha] \\ Q_2 &= [\bar{s}_\alpha \gamma_\mu (1 - \gamma_5) d] [\bar{u} \gamma^\mu (1 - \gamma_5) d]. \end{aligned} \quad (12)$$

The $\Delta I = \frac{1}{2}$ matrix elements can be expressed as [3]

$$\begin{aligned} \langle (\pi\pi)_0 | Q_1 | K^0 \rangle &= -\frac{1}{9} \sqrt{\frac{3}{2}} F_\pi (m_K^2 - m_\pi^2) B_1^{(1/2)} \\ \langle (\pi\pi)_0 | Q_2 | K^0 \rangle &= \frac{5}{9} \sqrt{\frac{3}{2}} F_\pi (m_K^2 - m_\pi^2) B_2^{(1/2)}, \end{aligned} \quad (13)$$

where $F_\pi = 132 \text{ MeV}$. The parameters $B_1^{(1/2)}$ and $B_2^{(1/2)}$ are both equal to 1 in the vacuum insertion approximation. In the $\frac{1}{N_c}$ approximation they are enhanced

[1] to approximately 5.2 and 2.2, respectively, at $\mu \approx .6 \text{ GeV}$, which corresponds to $B_2^{(1/2)}(m_c) \approx 2.8$. Qualitatively similar conclusions have been reached in refs. [2, 28].

A naive estimate of the resulting $\Delta I = \frac{1}{2}$ amplitude at zero'th order in QCD,

$$A_0^{V-A} \sim \frac{G_F}{\sqrt{2}} V_{ud} V_{us}^* \langle (\pi\pi)_0 | Q_2 | K^0 \rangle, \quad (14)$$

falls an order of magnitude short of experiment in the vacuum insertion approximation and a factor of 3 short in the $\frac{1}{N_c}$ approximation. The authors of [3] find, taking leading and next-to-leading order QCD corrections of the Wilson coefficients and matrix-elements in (11) into account, that phenomenologically building the $\Delta I = \frac{1}{2}$ amplitude into the standard model requires $B_2^{(1/2)}(m_c) \sim 6$. This is about a factor of 2 larger than obtained in the $\frac{1}{N_c}$ approximation [1], suggesting that there might be new contributions to the $\Delta I = \frac{1}{2}$ amplitude.

Next we summarize the status of the B meson semileptonic branching ratio in the standard model following the parton model analysis of ref. [7] and the recent discussion of ref. [12]. The semileptonic decay width of B mesons in the parton model is given to $\mathcal{O}(\alpha_s)$ by

$$\Gamma_\ell = \Gamma(b \rightarrow c \ell \bar{\nu}_\ell) = \Gamma_0 I_0\left(\frac{m_c^2}{m_b^2}, \frac{m_\ell^2}{m_b^2}, 0\right) \left[1 - \frac{2\alpha_s}{3\pi} f\left(\frac{m_c^2}{m_b^2}, \frac{m_\ell^2}{m_b^2}\right) + \mathcal{O}(\alpha_s^2)\right], \quad (15)$$

where

$$\Gamma_0 \equiv \frac{G_F^2 m_b^5 |V_{bc}|^2}{192\pi^3}, \quad (16)$$

and m_b is the pole mass. Expressions for the phase space factor I_0 for negligible electron or muon mass or non-negligible τ mass in the final state can be found in ref. [29]. The function f is given explicitly in ref. [30] and has been tabulated in ref. [31].

There are two classes of non-leptonic decays. For down and strange quarks in the final state one obtains

$$\Gamma(b \rightarrow c \bar{u} d) + \Gamma(b \rightarrow c \bar{u} s) = 3\Gamma_0 I_0\left(\frac{m_c^2}{m_b^2}, 0, 0\right) \eta J \quad (17)$$

For $\Gamma(b \rightarrow c \bar{c} s)$ one obtains an analogous expression with the substitution

$$I_0\left(\frac{m_c^2}{m_b^2}, 0, 0\right) \rightarrow I_0\left(\frac{m_c^2}{m_b^2}, 0, \frac{m_c^2}{m_b^2}\right) \quad (18)$$

In eq. (17) η is the leading-log anomalous dimension enhancement [8, 9] and J is the enhancement due to next-to-leading corrections [10, 11]. The total branching ratio

for charmless b decays in the standard model is expected to be $1 - 2\%$. We omit these decays from our discussion since they have a negligible effect on $\text{BR}_\ell(B)$ and n_c for our purposes.

The expected value of the semileptonic branching ratio depends strongly on m_b , m_c and Λ_{QCD} . Varying [22] m_b and m_c independently, the lowest value for $\text{BR}_\ell(B)$ is obtained for maximal m_b and minimal m_c ; keeping $m_b - m_c$ fixed $\text{BR}_\ell(B)$ increases with increasing m_b . In the parton model the electron spectrum in B decays implies [32] $m_b - m_c = 3.37 \pm .03 \text{ GeV}$, which is in good agreement with the difference obtained in HQET. The authors of ref. [33] have found that the B semileptonic decay rates imply $m_b \geq 4.66 \text{ GeV}$ and $m_c \geq 1.43 \text{ GeV}$ in HQET. Finally, recent lattice calculations [34] give $m_b = 4.94 \pm .15 \text{ GeV}$.

In Fig. 1 we plot parton model predictions for $\text{BR}_\ell(B)$ versus $\alpha_s(M_Z)$ at the renormalization point² $\mu = m_b$. We have checked that our plot is in good agreement with ref. [7] for $m_b = 4.6 \text{ GeV}$ and $m_c = 1.2 \text{ GeV}$. For less extreme choices of m_b and m_c one clearly expects $\text{BR}_\ell(B) > 12.5\%$. As an illustration, for $m_b = 4.8 \text{ GeV}$ and $m_c = 1.4 \text{ GeV}$ we obtain $\text{BR}_\ell(B) = 13.4\%$, (13%) for $\Lambda_{QCD}^{(4)} = 300 \text{ MeV}$, (400 MeV). This is to be contrasted with the measured values, which are substantially lower.

The authors of [12] have estimated non-perturbative $\mathcal{O}(1/m_b^2)$ and higher-order corrections to the parton model approximation in the heavy quark expansion and find a very small decrease, $\delta\text{BR}_\ell(B) \sim -.3\%$. Of course it may turn out that the operator product expansion fails for non-leptonic decays [13]. Although the total energy released is much larger than Λ_{QCD} , the energy per strongly interacting particle is considerably smaller than in semileptonic decays. This is especially relevant in the two charm decay channel where resonance effects may become important in the final hadronic state. However, the parton model $b \rightarrow c\bar{c}s$ decay rate would have to be doubled in order to obtain agreement with measurements of $\text{BR}_\ell(B)$. Of course, another possibility is that $\text{BR}_\ell(B)$ suppression is due to a combination of non-perturbative QCD effects and new physics.

Finally, we discuss the expected charm multiplicity for B decays in the parton model. The amount by which n_c exceeds 1 is identified with $BR(b \rightarrow c\bar{c}s)$. For example, for $m_b = 4.8 \text{ GeV}$, $m_c = 1.4 \text{ GeV}$, $\mu = m_b$ and $\alpha_s(M_Z) \approx .11 - .13$, we obtain $n_c \approx 1.2$. This essentially agrees with the heavy quark expansion results of

²For the expressions used in [7] ηJ is only μ independent to order α_s , reflecting our ignorance of order α_s^2 corrections. It was noted that for $\mu = m_b/2$ the QCD corrections are enhanced and one approaches the observed values of $\text{BR}_\ell(B)$. This is, however, an extreme possibility.

ref. [35], in which $n_c = 1.19 \pm .01$ is obtained for $m_b = 4.8 \text{ GeV}$, $m_c = 1.35 \text{ GeV}$, and $\alpha_s(M_W) = .12$. Lower values of m_c , while decreasing $\text{BR}_\ell(B)$ will increase n_c slightly.³ As already noted, the measured multiplicity is consistent with a small ‘charm deficit’. This would appear to rule out enhancement of the $b \rightarrow c\bar{c}s$ rate as the origin of $\text{BR}_\ell(B)$ suppression, and instead suggests that there are sizable new contributions to charmless b decays.

3. Phenomenology of the Quark Dipole Operators, and the Quark Mass Spectrum

This section is devoted to a model-independent discussion of the phenomenology of dipole penguin operators induced by new *flavor physics* in the context of the $\Delta I = \frac{1}{2}$ rule and $\text{BR}_\ell(B)$. In particular, we will determine what ranges for the operator coefficients correspond to significant enhancements of the $\Delta I = \frac{1}{2}$ amplitude and the B meson hadronic decay width. This, in turn, will have implications for the scale of new flavor physics which induces these diagrams, and for the associated induced quark masses and additional flavor-changing effects. The operator coefficients and induced masses are taken real throughout. We briefly remark on CP violation in the Conclusion.

We begin with discussion of the chromomagnetic dipole operators defined in eqs. (4), (5), and (6). Contributions of electromagnetic dipole operators to radiative B meson decays are discussed later. The relevant terms in the chromomagnetic dipole Lagrangian are shown explicitly below

$$\Delta\mathcal{L}_G = \sum_{i=+,-} C_G^{dsi}(\mu)Q_G^{dsi}(\mu) + \sum_{i=+,-} C_G^{sbi}(\mu)Q_G^{sbi}(\mu) + \sum_{i=+,-} C_G^{dbi}(\mu)Q_G^{dbi}(\mu) + H.c. + \dots (19)$$

The C_G are operator coefficients of dimension $(mass)^{-1}$. At leading order in QCD their evolution obeys the relation [36, 16, 18]

$$C_G^\pm(\mu_2) = \left(\frac{\alpha_s(\mu_2)}{\alpha_s(\mu_1)} \right)^{-\frac{2}{3b}} C_G^\pm(\mu_1), \quad (20)$$

where $b = 11 - 2n_g - 2/3n_f$. n_f is the number of flavors and n_g is the number of gluinos (0 or 1).⁴ The small anomalous dimension leads to a small decrease in

³For example, $m_c = 1.2 \text{ GeV}$ and $m_b = 4.6 \text{ GeV}$ gives $n_c \approx 1.25$.

⁴In supersymmetric models we will identify the scale of new physics with the squark masses and take the gluinos lighter than the squarks. We therefore do not include squark contributions to the β functions.

the coefficients of about 10% when evolving from TeV scales to the b scale. Unless otherwise specified, we use the following numerical inputs and thresholds for evolution of operator coefficients: $\Lambda_{QCD}^{(4)} = 300 \text{ MeV}$, $m_t = 170 \text{ GeV}$, $m_b = 4.8 \text{ GeV}$, and $m_c = 1.4 \text{ GeV}$.

The operator coefficients C_G^{ds+} , C_G^{sb+} and C_G^{db+} are also additively renormalized due to mixing with the standard model dimension-six operators at $\mathcal{O}(\alpha_s^2)$ [37]. The largest effect, due to mixing with Q_2 , changes C_G^{ds+} by $\mathcal{O}(3\%)$ and C_G^{sb+} by $\mathcal{O}(10\%)$, if these coefficients have magnitudes in the ranges of interest for $\Delta I = \frac{1}{2}$ enhancement and $\text{BR}_\ell(B)$ suppression. The relative sign of these contributions is not fixed. In the interest of simplicity we consider only the multiplicative renormalization and ignore these additional small corrections.

Parametrization of Flavor Physics

In general, each dipole operator coefficient might receive several new contributions. In the following analysis we parametrize the case in which there is a single source for all of the coefficients, corresponding to a single exchange of particles. Some examples are exchange of a single gluino-squark pair at one loop in supersymmetric theories, exchange of a single techniboson-technifermion pair in technicolor theories, and exchange of a quark-charged scalar pair in multi-Higgs doublet models. For a single exchange, the induced operator coefficient matrix and the induced quark mass matrix are proportional and of unit rank. It is straightforward to generalize to the case of several contributions, leading to matrices of rank 2 or 3.

We will deal with two quark basis, the quark mass eigenstates, or physical quarks, as usual denoted by d_L , s_L , etc., and the interaction basis quarks, which are denoted by d_L^i , d_R^i , $i = 1, 2, 3$. New interactions generate dipole coefficient matrices and quark mass matrices in the interaction basis. The physical transition dipole moments are obtained by taking matrix elements of these matrices in the mass eigenstate basis. In general, in the quark interaction basis we write $\Delta\mathcal{L}_G$ as

$$\Delta\mathcal{L}_G = \sum_{i,j} C_G^{ij}(\mu) Q_G^{ij}(\mu) + H.c., \quad (21)$$

where

$$Q_G^{ij} = g_s \bar{d}_L^i \sigma_{\mu\nu} t^a d_R^j G_a^{\mu\nu}. \quad (22)$$

The corresponding mass contributions, obtained by removing the gluons from the

dipole graphs, are

$$\Delta\mathcal{L}_{mass} = \sum_{i,j} \Delta m_{ij} \bar{d}_L^i d_R^j + H.c. \quad (23)$$

Restricting to the case of a single exchange of particles, we can parametrize the coefficients in the following way

$$C_G^{ij}(\mu) = \eta(\mu) \zeta_G \frac{\Delta m_{ij}(M)}{M^2}. \quad (24)$$

As noted above, C_G^{ij} and Δm_{ij} will be proportional rank 1 matrices. M is the scale of new physics, identified with the mass of the heaviest particle exchanged. In the supersymmetric examples it will be identified with the mass of the exchanged squark and in the technicolor examples it will be identified with the mass of the exchanged techniscalar. η is a dimensionless parameter which accounts for multiplicative renormalization from M down to hadronic mass scales, as discussed above. All of the flavor information is contained in the induced quark masses. The remaining model dependence is then represented by the flavor independent and μ -independent parameter ζ_G . Simple dimensional analysis reveals that the dipole operator coefficient must be $\mathcal{O}\left(\frac{\Delta m}{M^2}\right)$, so that ζ_G is nominally $\mathcal{O}(1)$. Indeed, in the supersymmetric case ζ_G typically varies between $\frac{1}{2}$ and 2, depending on the squark and gluino masses which enter the loop integrals, while in the technicolor case it is approximately $\frac{1}{2}$.

The induced quark masses associated with the transition dipole operators in eq. (19) are obtained by taking matrix elements of Δm_{ij} in the quark mass eigenstate basis. These are written as

$$\begin{aligned} \Delta\mathcal{L}'_{mass} = & \Delta m_{ds}^+ \bar{d}_L s_R + \Delta m_{ds}^- \bar{d}_R s_L + \Delta m_{sb}^+ \bar{s}_L b_R \\ & + \Delta m_{sb}^- \bar{s}_R b_L + \Delta m_{db}^+ \bar{d}_L b_R + \Delta m_{db}^- \bar{d}_R b_L + H.c. \end{aligned} \quad (25)$$

The physical dipole operator coefficients are given in terms of these masses by

$$C_G^{sb\pm}(\mu) = \eta(\mu) \zeta_G \frac{\Delta m_{sb}^\pm(M)}{M^2}, \quad C_G^{db\pm}(\mu) = \eta(\mu) \zeta_G \frac{\Delta m_{db}^\pm(M)}{M^2} \quad (26)$$

$$C_G^{ds\pm}(\mu) = \eta(\mu) \zeta_G \frac{\Delta m_{ds}^\pm(M)}{M^2}. \quad (27)$$

Given several contributions to the dipole operator coefficients each of them can be parametrized as above, although in general M and ζ_G will differ in each case.

The ranges for the induced quark masses in (27) which would strongly suggest a connection to the observed quark mass spectrum are found by expressing these

masses in terms of the interaction basis entries, Δm_{ij} . This is straightforward given reasonably general assumptions about the hierarchy obeyed by entries of the full down quark mass matrix in the interaction basis.⁵ Details are provided in Appendix A. Given the hierarchy of eq. (A1) one concludes the following:⁶

(a) If $|\Delta m_{ds}^+| \sim |\theta_c m_s|$ ($\sim 33 \text{ MeV}$) then the induced unit-rank mass matrix, Δm_{ij} , can be associated with generation of the bulk of θ_c or m_s , but not both.

(b) If $|\Delta m_{sb}^+| \sim |V_{cb} m_b|$ ($\sim 230 \text{ MeV}$) then Δm_{ij} can be associated with generation of the bulk of V_{cb} or m_b , but not both.

(c) If $|\Delta m_{db}^+| \sim |V_{ub} m_b|$ ($\sim 23 \text{ MeV}$) then Δm_{ij} can, in general, be associated with generation of the bulk of V_{ub} , V_{cb} , or m_b , but not all three.

The question of which features of the quark mass spectrum are in fact generated in (a)-(c) above is a model-dependent issue which we address when discussing specific examples. In principle, all of the KM angles and down quark masses can be associated with induced dipole operator coefficients given several sources for these operators.

With the above parametrization we can study $\Delta I = \frac{1}{2}$ enhancement and $\text{BR}_\ell(B)$ suppression due to new flavor physics in a model-independent way in the appropriate $(\zeta_G \Delta m, M)$ plane. Two model-independent conditions constrain the allowed regions of $\Delta I = \frac{1}{2}$ enhancement and $\text{BR}_\ell(B)$ suppression in these planes:

(i) The scale of new flavor physics should lie above the weak scale in order to have avoided detection.

(ii) The induced quark masses should not spoil the observed quark mass hierarchy. Since ζ_G is nominally of $\mathcal{O}(1)$ this means that $\zeta_G \Delta m$ should not be much larger than the corresponding range in (a)-(c) above in order to avoid fine-tuning of the quark mass spectrum.⁷

We will see that $\text{BR}_\ell(B)$ suppression and $\Delta I = \frac{1}{2}$ enhancement of a reasonable magnitude can be obtained with $\zeta_G \sim 1$ and induced masses in the ranges specified

⁵There will be some uncertainty due to possible cancelations among different sources of quark mass and between up and down sector contributions to the KM angles.

⁶The numbers in parenthesis, evaluated at $\mu = m_c$, are illustrative and correspond to the running masses $m_c(m_c) = 1.4 \text{ GeV}$, $m_b(m_c) = 5.4 \text{ GeV}$ (or $m_b(m_b) \approx 4.25 \text{ GeV}$), $m_s(m_c) = 150 \text{ MeV}$, and $V_{cb} = .043$, $|V_{ub}/V_{cb}| = .1$.

⁷For example, the amount of tuning of θ_c or m_s associated with the magnitude of Δm_{ds}^+ is of order one part in $|\frac{\Delta m_{ds}^+}{\theta_c m_s}|$.

in (a)-(c) above. This implies that, in general, a connection with the observed quark mass spectrum is possible. Specific models can be classified according to where they lie in the planes of Δm vs. M , or according to whether such a connection can be realized. Flavor-changing constraints will rule out parts of the planes and one has to make sure that the models survive these restrictions.

The B Meson Semileptonic Branching Ratio

We begin with discussion of $\text{BR}_\ell(B)$. Estimates in the B system are more reliable and easier to present. The parton model contribution of the dipole operators $Q_G^{sb\pm}$ to the inclusive hadronic decay width of B mesons is given by

$$\Gamma(b \rightarrow sg) = \frac{4}{3} \alpha_s(m_b) m_b^3 \left(|C_G^{sb+}(m_b)|^2 + |C_G^{sb-}(m_b)|^2 \right). \quad (28)$$

In terms of our parametrization this is

$$\Gamma(b \rightarrow sg) = \frac{4}{3} \eta^2(m_b) \alpha_s(m_b) m_b^5 |V_{cb}|^2 \frac{\zeta_G^2}{M^4} (\Delta m_{sb}^+(M)^2 + \Delta m_{sb}^-(M)^2). \quad (29)$$

Expressions for the contribution of $Q_G^{db\pm}$ to $\Gamma(b \rightarrow dg)$ are analogous, with s indices replaced everywhere by d indices. The inclusive gluon channel decay width, $\Gamma(b \rightarrow xg)$, is proportional to

$$C_G^{sb+2} + C_G^{sb-2} + C_G^{db+2} + C_G^{db-2} \quad (30)$$

evaluated at m_b . If there is only one source or exchange of particles giving rise to the dipole operators then it is also proportional to

$$\Delta m'^2 \equiv \Delta m_{sb}^{+2} + \Delta m_{sb}^{-2} + \Delta m_{db}^{+2} + \Delta m_{db}^{-2}, \quad (31)$$

evaluated at M .

In order to study the connection to the quark mass spectrum it is convenient to parametrize $\Delta m'$ as

$$\Delta m'(\mu) = \xi' |V_{cb} m_b(\mu)|, \quad (32)$$

where ξ' is a μ -independent dimensionless parameter. For illustrative purposes we assume that $|C_G^{sb-}| \lesssim |C_G^{sb+}|$, $|C_G^{db-}| \lesssim |C_G^{db+}|$ or, equivalently, that $|\Delta m_{sb}^-| \lesssim |\Delta m_{sb}^+|$,

$|\Delta m_{db}^-| \lesssim |\Delta m_{db}^+|$.⁸ According to our previous discussion there are then two regions of interest for ξ' (or $\Delta m'$):

Case (I) $\xi' \sim 1$ (or $\Delta m' \sim |V_{cb}m_b|$), taken together with the small V_{ub} to V_{cb} ratio, suggests the hierarchy

$$|\Delta m_{sb}^+| \sim |V_{cb}m_b|, \quad |\Delta m_{db}^+| \sim |V_{ub}m_b|. \quad (33)$$

So $\xi' \sim 1$ can be associated with generation of V_{cb} or m_b .

Case (II) $\xi' \sim .1$ (or $\Delta m' \sim |V_{ub}m_b|$) is consistent with

$$|\Delta m_{db}^+| \sim |V_{ub}m_b|, \quad |\Delta m_{sb}^+| \sim |V_{ub}m_b|. \quad (34)$$

So $\xi' \sim .1$ can be associated with generation of V_{ub} . Alternatively, $\xi' \sim .1$ can be associated with generation⁹ of V_{cb} in conjunction with m_b . Details are given in Appendix A, see eq. (A6).

In Fig. 2 we plot contours for $\text{BR}_\ell(B) = 10\%$ and 11% in the $(|\zeta_G \xi'|, M)$ plane. $\eta(m_b)$ has been obtained with non-supersymmetric β -functions but it is nearly the same in supersymmetric models. Note that large uncertainties in $\text{BR}_\ell(B)$ due to lack of precise knowledge of V_{cb} and m_b conveniently drop out in this parametrization since the gluon channel decay width is proportional to $m_b^5 V_{cb}^2$, like the standard model decay widths. The parton model charm multiplicities for Fig. 2 are $n_c = .9$ ($\text{BR}_\ell(B) = 10\%$) and $n_c = 1.0$ ($\text{BR}_\ell(B) = 11\%$). The latter is in better agreement with the measured charm multiplicity than the standard model prediction. The inclusive gluon channel branching ratios are $\text{BR}(b \rightarrow xg) = 25\%$ ($\text{BR}_\ell(B) = 10\%$) and 18% ($\text{BR}_\ell(B) = 11\%$), about an order of magnitude above the standard model prediction.¹⁰

⁸If instead $\Delta m_{sb}^- \gg \Delta m_{sb}^+$ and $\Delta m_{db}^- \gg \Delta m_{db}^+$, which does not necessarily spoil the quark mass spectrum, then the scale of new physics associated with $\text{BR}_\ell(B)$ suppression is increased but the connection to the KM matrix is lost.

⁹In this case the induced mass matrix is assumed to account for the bulk of m_{23}^d and m_{33}^d , leading to suppression of Δm_{sb}^+ .

¹⁰If $\text{BR}_\ell(B)$ suppression is due to a combination of new physics and non-perturbative enhancement of $\Gamma(b \rightarrow c\bar{c}s)$ then n_c would be increased and $\text{BR}(b \rightarrow xg)$ would be decreased. For example, keeping $\text{BR}_\ell(B)$ fixed at 11% , a 20% enhancement of the two charm decay rate would shift n_c by $\approx +.05$ and $\text{BR}(b \rightarrow xg)$ by $\approx -7\%$. However, our conclusions concerning quark mass generation would not change qualitatively.

From Fig. 2 it is clear that the desired $\text{BR}_\ell(B)$ suppression can, in principle, take place in either region of ξ' of relevance to the quark mass spectrum.

- Case (I) corresponds to a scale of new physics $M \sim 1 - 2 \text{ TeV}$. Henceforth, we refer to this scale of new physics as **Region I**. In this case $\Gamma(b \rightarrow dg) \ll \Gamma(b \rightarrow sg)$.
- Case (II) corresponds to a somewhat lower scale of new physics $M \sim 300 - 700 \text{ GeV}$. Henceforth, we refer to this scale of new physics as **Region II**. In this case $\Gamma(b \rightarrow dg) \lesssim \Gamma(b \rightarrow sg)$ is possible.

We will discuss specific examples of new flavor physics which feature considerable overlap with one or the other region of the $(\Delta m', M)$ plane. But first we discuss what is potentially the most restrictive flavor-changing constraint associated with B hadronic decay enhancement.

$b \rightarrow s\gamma$ and $b \rightarrow d\gamma$

In general, enhancement of the B meson hadronic decay width will be correlated with contributions to $\text{BR}(b \rightarrow s\gamma)$ or $\text{BR}(b \rightarrow d\gamma)$ due to the induced electromagnetic dipole operators

$$\begin{aligned} Q_F^{sb\pm} &= eQ_d \bar{s} \sigma_{\mu\nu} \frac{1 \pm \gamma_5}{2} b F^{\mu\nu} \\ Q_F^{db\pm} &= eQ_d \bar{d} \sigma_{\mu\nu} \frac{1 \pm \gamma_5}{2} b F^{\mu\nu}, \end{aligned} \quad (35)$$

where Q_d is the electric charge of the down quark. An important question is whether the hadronic enhancement associated with $\text{BR}_\ell(B)$ is consistent with the CLEO bound on the inclusive radiative branching ratio, the sum of $\text{BR}(b \rightarrow s\gamma)$ and $\text{BR}(b \rightarrow d\gamma)$. The answer is model-dependent and we will give a general criterion which can be used to distinguish those models in which the contribution of new physics is not too large. On the other hand, $B_d - \bar{B}_d$ mixing constraints are not restrictive, as will become clear when we discuss specific examples.

The Lagrangian for electromagnetic dipole operators is

$$\Delta\mathcal{L}_F = C_F^{sb+} Q_F^{sb+} + C_F^{sb-} Q_F^{sb-} + C_F^{db+} Q_F^{db+} + C_F^{db-} Q_F^{db-} + H.c. \quad (36)$$

Note that in general the relative sign between new physics contributions to C_F^{sb+} and the standard model contribution to C_F^{sb+} is not fixed and they can interfere destructively or constructively. In attempting to determine which models do not give dangerously large contributions to the inclusive radiative branching ratio we

can ignore the standard model contribution. This will not alter our conclusions qualitatively.

At leading-order, renormalization of the operator coefficients is given by [37]

$$C_F^\pm(\mu_2) = \left(\frac{\alpha_s(\mu_2)}{\alpha_s(\mu_1)}\right)^{-\frac{4}{3b}} C_F^\pm(\mu_1) + 2 \left[\left(\frac{\alpha_s(\mu_2)}{\alpha_s(\mu_1)}\right)^{-\frac{4}{3b}} - \left(\frac{\alpha_s(\mu_2)}{\alpha_s(\mu_1)}\right)^{-\frac{2}{3b}} \right] C_G^\pm(\mu_1). \quad (37)$$

Again we ignore mixing with the standard model four-fermion operator Q_2 since the resulting contribution to $\text{BR}(b \rightarrow s\gamma)$ is essentially the same as in the standard model. The relative sign between C_F^+ and C_G^+ , or C_F^- and C_G^- is model dependent and renormalization due to mixing with the chromomagnetic dipole operators can be constructive or destructive.

Applying our parametrization for a single source for dipole operators to the electromagnetic dipole operator coefficients gives

$$C_F^{sb\pm}(M) = \zeta_F \frac{\Delta m_{sb}^\pm(M)}{M^2} \text{ GeV}^{-1}, \quad C_F^{db\pm}(M) = \zeta_F \frac{\Delta m_{sb}^\pm(M)}{M^2} \text{ GeV}^{-1}. \quad (38)$$

ζ_F is a dimensionless, μ -independent parameter which is the analog of ζ_G for photon emission. Again, all of the flavor dependence is contained in the induced quark masses.

The inclusive decay width for $b \rightarrow s\gamma$ is given by

$$\Gamma(b \rightarrow s\gamma) = \alpha_{em} Q_d^2 m_b^3 (|C_F^{sb+}(m_b)|^2 + |C_F^{sb-}(m_b)|^2). \quad (39)$$

$\Gamma(b \rightarrow d\gamma)$ is analogous, with s indices again replaced by d indices. The total B radiative decay width is proportional to

$$C_F^{sb+2} + C_F^{sb-2} + C_F^{db+2} + C_F^{db-2}, \quad (40)$$

evaluated at m_b .

To arrive at a model-independent criterion which insures that the radiative branching ratio will not be too large we need to determine what is a sufficiently small magnitude for the ratio $\frac{\zeta_F}{\zeta_G}$, given that $\Gamma(b \rightarrow xg)$ gives the desired $\text{BR}_\ell(B)$ suppression. In Fig. 3 we plot this ratio for several representative values of $\text{BR}_\ell(B)$ and $\text{BR}(b \rightarrow x\gamma)$.¹¹ We have used non-supersymmetric β -functions above m_t , but the supersymmetric case is nearly the same, again exhibiting a weak scale dependence. Results have been included for ζ_F and ζ_G of same, or opposite sign.

¹¹We have evolved the chromomagnetic and electromagnetic dipole operator coefficients from m_b to M in order to determine this ratio.

The ratio $\frac{\zeta_F}{\zeta_G}$ is a model-dependent quantity which, in general, will depend on the charges of the particles which radiate the photon, ratios of loop integrals, etc. Essentially, what we find from Fig. 3 is that *models which give the desired $\text{BR}_\ell(B)$ suppression should satisfy*

$$|\zeta_F| < |\zeta_G| \tag{41}$$

in order to insure that new contributions to $\text{BR}(b \rightarrow x\gamma)$ are sufficiently small. It is important to realize that $\text{BR}(b \rightarrow d\gamma)$ provides a very large window for new physics, since it is two orders of magnitude smaller than $\text{BR}(b \rightarrow s\gamma)$ in the standard model. In fact, in those models in which $\text{BR}_\ell(B)$ suppression takes place in Region II, $\text{BR}(b \rightarrow d\gamma) \sim (1 - 1) \times 10^{-4}$ is likely since Δm_{db}^\pm and Δm_{sb}^\pm tend to be of same order, see eq. (34).

If the chromomagnetic and electromagnetic dipole operators are due to gluon and photon emission from the same particle of charge Q , then $\frac{\zeta_F}{\zeta_G} = \frac{Q}{Q_d}$, where $Q_d = -\frac{1}{3}$. This implies that in multi-Higgs doublet models of $\text{BR}_\ell(B)$ suppression, ζ_F is larger in magnitude than ζ_G because the dominant loop integral for photon emission corresponds to radiation from the charge $\frac{2}{3}$ top quark. Therefore, one can not simultaneously obtain the desired hadronic width enhancement and satisfy the CLEO bound. Similarly, one can rule out E_6 -motivated models of $\text{BR}_\ell(B)$ suppression in which the chromomagnetic dipole operators are due to penguin graphs with scalar diquarks and a top quark in the loop. The case of dipole penguin graphs with neutral scalars and vectorlike quarks in the loop is borderline. Since the photon and gluon are both emitted from charge $-\frac{1}{3}$ vectorlike down quarks, $\zeta_F = \zeta_G$ and modest destructive interference with the standard model penguin contribution would be required. Although potentially interesting, we will not discuss this model further.

In the supersymmetric examples which we consider, a gluino and squark are exchanged at one loop. ζ_F will be smaller in magnitude than ζ_G because the loop integral for photon emission, corresponding to emission from the squark, is significantly smaller than the dominant loop integral for gluon emission, corresponding to emission from the gluino. In the technicolor examples which we consider, $|\frac{\zeta_F}{\zeta_G}| \approx \frac{1}{2}$ because both the photon and gluon are emitted from a techniscalar with charge $\frac{1}{6}$, or $\frac{|Q_d|}{2}$. We will see explicitly in Sections 4 and 5 that $b \rightarrow s\gamma$ and $b \rightarrow d\gamma$ constraints

are not very restrictive in these examples.

The $\Delta I = \frac{1}{2}$ Amplitude

As already noted, it is difficult to estimate the $K^0 \rightarrow \pi\pi$ amplitude induced by the dipole operators $Q_G^{ds\pm}$. The lowest order representation of $Q_G^{ds\pm}$ in the chiral lagrangian vanishes due to an exact cancelation at leading order in chiral perturbation theory between the direct $K \rightarrow \pi\pi$ amplitude and a pole contribution combining the strong interaction $KK\pi\pi$ vertex and the K -vacuum tadpole [21, 38]. This can be seen directly by using PCAC soft pion theorems to relate the $K \rightarrow \pi\pi$ and $K \rightarrow$ vacuum matrix elements of $Q_G^{ds\pm}$. The reason for this cancelation is that the lowest order representation is similar in form to the mass term in the strong interaction lagrangian. As a result, it can be rotated away by a chiral transformation without inducing any other $\Delta S = 1$ terms in the lagrangian.

The leading-order chiral representation of $\Delta\mathcal{L}_G$ for $K \rightarrow \pi\pi$ decay arises at $\mathcal{O}(p^4)$ and is of the form [21]

$$\frac{a}{\Lambda^2} Tr[\lambda_6 U \partial_\mu U^\dagger \partial^\mu U] + H.c., \quad (42)$$

where Λ is of order the chiral symmetry breaking scale, $\Lambda_{\chi SB}$. Following ref. [21] we make a crude estimate of the resulting $\Delta I = \frac{1}{2}$ amplitude by assuming that it is suppressed by $\frac{p^2}{\Lambda^2} \approx \frac{m_K^2}{\Lambda^2}$ relative to the ‘direct’ PCAC $K \rightarrow \pi\pi$ amplitude. We write it as

$$A_0 = (C_G^{ds+}(\mu) - C_G^{ds-}(\mu)) \langle (\pi\pi)_0 | Q_G^{ds+}(\mu) | K^0 \rangle \frac{m_K^2}{\Lambda^2}. \quad (43)$$

Although we expect $\Lambda_{\chi SB} \sim 1 \text{ GeV}$ [39, 40], Λ can vary substantially, in general, for higher order chiral lagrangian contributions, depending on which process or diagram is being considered. The suppression factor in eq. (43) could, a priori, lie anywhere in the interval $\frac{m_K^2}{\Lambda^2} \sim .1 - .4$. This is certainly the case for higher-order contributions to the $\Delta I = \frac{1}{2}$ rule in the standard model [41, 42]. We will therefore present all of our results for the $\Delta I = \frac{1}{2}$ amplitude in terms of $\frac{m_K^2}{\Lambda^2}$, keeping it as a phenomenological parameter to be determined in the future.

We use a PCAC calculation [43] of the ‘direct’ matrix element in eq. (43), which gives

$$\langle (\pi\pi)_0 | Q_G^{ds+} | K^0 \rangle = -\sqrt{\frac{3}{2}} \frac{m_0^2}{2} \frac{m_K^2}{m_u + m_s} \frac{F_K}{F_\pi^2} B_G^{(1/2)}. \quad (44)$$

The decay constants are $F_\pi = 132 \text{ MeV}$ and $F_K = 161 \text{ MeV}$. m_0^2 parametrizes the relevant mixed condensate,

$$g_s \langle 0 | \bar{q} \sigma_{\mu\nu} T^a G_a^{\mu\nu} q | 0 \rangle = m_0^2 \langle 0 | \bar{q} q | 0 \rangle, \quad (45)$$

and $B_G^{(1/2)}$ is a dimensionless matrix element parameter which is approximately equal to 1.¹² The two most recent determinations of m_0^2 are a lattice calculation [44] and a fit using QCD sum rules and B -meson data [45], which give $m_0^2(m_c) \approx 1 \text{ GeV}^2$ for $m_c = 1.4 \text{ GeV}$, or

$$\langle (\pi\pi)_0 | Q_G^{ds+} | K^0 \rangle \approx -9 \text{ GeV}^2 \quad (46)$$

for $m_s(m_c) = 150 \text{ MeV}$. We will make use of this result throughout and evaluate the operator coefficients in eq. (43) at m_c .

In order to uncover a possible connection between $\Delta I = \frac{1}{2}$ amplitude enhancement and generation of θ_c or m_s it is useful to parametrize the induced masses in eq. (27) as

$$\Delta m_{ds}^\pm(\mu) = \xi_{ds}^\pm |\theta_c m_s(\mu)|, \quad (47)$$

where, as usual, ξ_{ds}^\pm are dimensionless μ -independent parameters. According to our previous discussion of induced masses, generation of θ_c or m_s would correspond to $\xi_{ds}^+ \sim 1$.

In terms of our parametrization, the $\Delta I = \frac{1}{2}$ amplitude is given by

$$A_0 = \frac{\zeta_G (\xi_{ds}^+ - \xi_{ds}^-) \eta(m_c) \theta_c m_s(M)}{M^2} \langle (\pi\pi)_0 | Q_G^{ds+} | K^0 \rangle \frac{m_K^2}{\Lambda^2}. \quad (48)$$

It is important to point out that comparison of the observed $\Delta I = \frac{1}{2}$ and $\Delta I = \frac{3}{2}$ amplitudes in $K \rightarrow 3\pi$ decays and $K \rightarrow 2\pi$ decays constrains the chiral structure of the $\Delta I = \frac{1}{2}$ amplitude [46]. In particular, current algebra relations imply that the contribution of Q_G^{ds-} to the $K \rightarrow \pi\pi$ amplitude¹³ should be small, perhaps $\lesssim 10\%$. Equivalently, if the dipole operators account for 30% – 50% of the $\Delta I = \frac{1}{2}$ amplitude then

$$\left| \Delta m_{ds}^+ \right| \gtrsim (2 - 4) \left| \Delta m_{ds}^- \right|, \quad (49)$$

¹²The authors of ref. [43] take $B_G^{(1/2)}(m_c) = 1$, based on the assumption that it is reasonable to evaluate the matrix element at m_c .

¹³I would like to thank John Donoghue for bringing this point and ref. [46] to my attention.

or $|\xi_{ds}^+| \gtrsim (2 - 4) |\xi_{ds}^-|$ should be satisfied.

In Fig. 4 we plot contours of constant R_0 , defined as the ratio of magnitudes of the dipole induced $\Delta I = \frac{1}{2}$ amplitude, A_0 , to the observed $\Delta I = \frac{1}{2}$ amplitude A_0^{exp} ,

$$R_0 \equiv \left| \frac{A_0}{A_0^{exp}} \right|, \quad (50)$$

in the plane of $|\zeta_G(\xi_{ds}^+ - \xi_{ds}^-)|$ vs. M . To first approximation, the vertical axis in Fig. 4 can be identified with $|\zeta_G \xi_{ds}^+|$ for large $\Delta I = \frac{1}{2}$ enhancements. Again, η is nearly the same in supersymmetric models. For purposes of comparison we have also reproduced contours of $\text{BR}_\ell(B)$ from Fig. 2 in the $(|\zeta_G \xi^+|, M)$ plane.

Our model-independent analysis reveals that $\zeta_G \Delta m_{ds}^+ \approx \theta_c m_s$ together with $R_0 \approx (1 - 1.5) \frac{m_K^2}{\Lambda^2}$ can be obtained in the $M \sim \frac{1}{2} \text{ TeV}$ region, identified as Region II in our discussion of $\text{BR}_\ell(B)$. In general, we expect $\zeta_G \sim 1$ so that we can associate this region with generation of θ_c or m_s . If m_K^2/Λ^2 lies in the range .2 - .4, generation of 30% - 60% of the observed $\Delta I = \frac{1}{2}$ amplitude is possible. Since the relative sign between the standard model 4-quark operator contribution and new dipole operator contributions to the $\Delta I = \frac{1}{2}$ amplitude is generally not fixed, the two could add constructively helping to account for the entire $\Delta I = \frac{1}{2}$ amplitude.

In the next two sections we will discuss supersymmetric and techniscalar models. In particular, we will see that in both cases substantial overlap with the above region of Fig. 4 is not ruled out by the small value of $m(K_L) - m(K_S)$, although in the supersymmetric examples a modest one part in two or three tuning may be required for the larger $\Delta I = \frac{1}{2}$ amplitudes. Gluinos in the ‘light-gluino’ window will constitute a special case. Because of the extreme ratio of gluino to squark masses entering the relevant loop integral, ζ_G will be substantially larger than 1. The induced quark masses will generally be too small to be of significance, but very large $\Delta I = \frac{1}{2}$ amplitudes will be possible for squark masses below 500 GeV.

To summarize, we have performed a model-independent analysis of potential contributions of chromomagnetic dipole operators to the B hadronic decay width and the $(\Delta I = \frac{1}{2}) K \rightarrow \pi\pi$ amplitude. By comparing results for $\Delta I = \frac{1}{2}$ enhancement and $\text{BR}_\ell(B)$ suppression in Fig. 4 we can loosely identify two interesting scales of new physics, or M .

- In *Region I*, corresponding to $M \sim 1 - 2 \text{ TeV}$, the desired $\text{BR}_\ell(B)$ suppression can be directly associated with generation of V_{cb} or m_b (but not both). However,

substantial $\Delta I = \frac{1}{2}$ enhancement would lead to undesirably large contributions to θ_c or m_s .

- In *Region II*, corresponding to $M \sim \frac{1}{2} TeV$, the desired $BR_\ell(B)$ suppression can be directly associated with generation of V_{ub} , or with generation of V_{cb} in conjunction with m_b . The magnitude of the induced $\Delta I = \frac{1}{2}$ amplitude is difficult to estimate. However, it can be as large as 30% to 60% of the observed amplitude, without resorting to unreasonably large matrix elements. Furthermore, it can be directly associated with generation of θ_c or m_s . The question of which masses or mixing angles are actually generated in Region I or Region II is model-dependent.

- Finally, we have given a general criterion which can be used to distinguish those models of $BR_\ell(B)$ suppression in which the branching ratios for $b \rightarrow s\gamma$ and $b \rightarrow d\gamma$ are not too large. We have also argued that in Region II it is possible to obtain $BR(b \rightarrow d\gamma) \approx 10^{-4}$, a dramatic departure from the standard model prediction.

We are now ready to discuss models which illustrate the above points explicitly.

4. Supersymmetry

In this section we will discuss the phenomenology of radiatively induced dipole operators in supersymmetric models. We begin by setting some notation. Superpartners are denoted by tildes. For example, the gluino mass is $m_{\tilde{g}}$. Left-handed and right-handed down squarks are denoted by $\tilde{d}_L^i, \tilde{d}_R^i, i = 1, 2, 3$ in the quark interaction basis, and by $\tilde{d}_L, \tilde{d}_R, \tilde{s}_L, \tilde{s}_R, \tilde{b}_L, \tilde{b}_R$ in the physical quark basis. We make the usual assumption of an approximately degenerate or universal flavor-diagonal squark masses, $m_{\tilde{q}}^2$, corresponding to the following terms in the squark mass matrix,

$$\sum_{i=1,2,3} m_{\tilde{q}}^2 (\tilde{d}_L^{i*} \tilde{d}_L^i + \tilde{d}_R^{i*} \tilde{d}_R^i). \quad (51)$$

Deviations from universality are of two types. Additional non-universal left-left and right-right squark masses

$$\sum_{ij} \delta \tilde{m}_{i_L j_L}^2 \tilde{d}_L^{i*} \tilde{d}_L^j + \sum_{ij} \delta \tilde{m}_{i_R j_R}^2 \tilde{d}_R^{i*} \tilde{d}_R^j, \quad (52)$$

generally lead to off-diagonal squark masses in the quark mass eigenstate basis. Left-right squark masses,

$$\sum_{ij} \delta \tilde{m}_{i_L j_R}^2 \tilde{d}_L^{i*} \tilde{d}_R^j + H.c., \quad (53)$$

are obtained from scalar trilinear couplings to Higgs doublets. In general, these also lead to off-diagonal squark masses in the quark mass eigenstate basis¹⁴,

$$\delta\tilde{m}_{d_L s_R}^2 \tilde{d}_L^* \tilde{s}_R + \delta\tilde{m}_{d_L b_R}^2 \tilde{d}_L^* \tilde{b}_R + \delta\tilde{m}_{s_L b_R}^2 \tilde{s}_L^* \tilde{b}_R + L \longleftrightarrow R. \quad (54)$$

The assumption of near degeneracy of down squark masses, generally required by flavor-changing neutral current (FCNC) constraints¹⁵ [47] for $m_{\tilde{q}}$ and $m_{\tilde{g}}$ of a TeV or less, corresponds to $\delta\tilde{m}^2 \ll m_{\tilde{q}}^2$. This allows us to work in the squark mass insertion approximation when computing radiative flavour-changing effects. We neglect CP violation and take all masses and operator coefficients to be real.

We will be interested in contributions to the chromomagnetic dipole operators which are generated by the gluino penguin graphs of Fig. 5.¹⁶ These graphs were first studied in ref. [50] in the context of potential contributions to ϵ'/ϵ and have also been studied in the context of b decays [51]. The resulting chromomagnetic dipole operator coefficients in the quark interaction basis, see eqs. (21), (22), are given at $\mathcal{O}(\delta\tilde{m}^2/m_{\tilde{q}}^2)$ by

$$C_G^{ij}(m_{\tilde{q}}) = \frac{\alpha_s x}{8\pi m_{\tilde{g}}} \left(3E(x) - \frac{16}{3}C(x) \right) \frac{\delta\tilde{m}_{i_L j_R}^2}{m_{\tilde{q}}^2}, \quad (55)$$

where $x = m_{\tilde{g}}^2/m_{\tilde{q}}^2$, (at $m_{\tilde{q}}$). The loop integrals $E(x)$ and $C(x)$, corresponding to vector boson emission from the gluino and squark lines, respectively, are given by

$$E(x) = \frac{1}{(1-x)^3} [2(1-x) + (1+x)\ln x] \quad (56)$$

$$C(x) = \frac{1}{4(1-x)^4} [5x^2 - 4x - 1 - 2x(x+2)\ln x]. \quad (57)$$

Associated radiative contributions to the down quark mass matrix in the quark interaction basis, see eq. (23), are given at $\mathcal{O}(\delta\tilde{m}^2/m_{\tilde{q}}^2)$ by

$$\Delta m_{ij}(m_{\tilde{q}}) = \frac{4}{3} \frac{\alpha_s}{2\pi} \frac{\delta\tilde{m}_{i_L j_R}^2}{m_{\tilde{q}}^2} m_{\tilde{g}} \frac{(x \ln x + 1 - x)}{(1-x)^2}. \quad (58)$$

¹⁴In general, the quark and left-right squark mass matrices will not be proportional

¹⁵Strictly speaking, near degeneracy is required among the left-handed squarks and among the right-handed squarks separately. The degeneracy requirement can be satisfied [48] or relaxed [49] in models with horizontal symmetries.

¹⁶Neutralino penguin contributions are suppressed by $\mathcal{O}(\frac{\alpha_{em}}{\alpha_s})$. Chargino and charged Higgs dipole penguin contributions to the $\Delta I = \frac{1}{2}$ amplitude and $\text{BR}_\ell(B)$ suppression must also be substantially smaller in the MSSM due to various factors, including small Yukawa couplings and FCNC constraints.

Radiatively induced dipole operator coefficients and quark masses in the physical quark basis are given in terms of the corresponding left-right squark mass matrix entries. For example,

$$C_G^{ds+}(m_{\tilde{q}}) = \frac{\alpha_s x}{8\pi m_{\tilde{g}}} \left(3E(x) - \frac{16}{3}C(x) \right) \frac{\delta\tilde{m}_{dLsR}^2}{m_{\tilde{q}}^2} \quad (59)$$

$$\Delta m_{ds}^+ = \frac{4}{3} \frac{\alpha_s}{2\pi} \frac{\delta\tilde{m}_{dLsR}^2}{m_{\tilde{q}}^2} m_{\tilde{g}} \frac{(x \ln x + 1 - x)}{(1-x)^2}. \quad (60)$$

The loop integrals $E(x)$ and $C(x)$ correspond to gluon emission from the gluino and squark lines, respectively. C_G^{ds-} and Δm_{ds}^- are obtained via the substitution $\delta\tilde{m}_{dLsR}^2 \rightarrow \delta\tilde{m}_{dRsL}^2$. Expressions for the other chromomagnetic dipole operator coefficients and quark masses in eqs. (19) and (25) are completely analogous.

Note that whereas our model-independent analysis was restricted to the case of a single exchange of particles in the loop, up to six squark mass eigenstates can be exchanged in the supersymmetric loops, leading to matrices C_G^{ij} and Δm_{ij} which are generally rank 3. Nevertheless, to good approximation these two matrices are proportional, given approximately degenerate squark masses. Deviations from proportionality first arise at $\mathcal{O}(\delta\tilde{m}^4/m_{\tilde{q}}^4)$ and can be neglected for our purposes. The supersymmetric results can therefore be recast in terms of our model-independent parametrization, as in eq. (24). In particular, ζ_G is given in terms of ratios of loop integrals and is flavor independent, depending only on $m_{\tilde{g}}$ and $m_{\tilde{q}}$. The scale of new physics, M , is identified with the larger of the two masses. As will become clear below, maximization of the $\Delta I = \frac{1}{2}$ amplitude favors $m_{\tilde{q}} \gg m_{\tilde{g}}$ so that M will be identified with the squark mass scale.

The $\Delta I = \frac{1}{2}$ Amplitude.

We begin by estimating upper bounds on the dipole induced $\Delta I = \frac{1}{2}$ amplitude implied by the observed mass difference, Δm_K^{exp} . The relevant supersymmetric contributions [52, 53, 54] to Δm_K are given in eq. (B1) of Appendix B. The matrix elements are evaluated in the vacuum insertion approximation with m_s and m_d taken at m_c . We choose $m_s = 150 \text{ MeV}$ and $m_d = 8 \text{ MeV}$. α_s and the supersymmetric mass parameters are taken at the squark mass scale, $m_{\tilde{q}}$, and QCD running of the $\Delta S = 2$ operator coefficients to hadronic scales is not included. These are clearly only order of magnitude estimates and a more sophisticated treatment taking into account QCD corrections and a more rigorous determination of the matrix elements is left for future work.

The first three terms in eq. (B1) depend on the same squark mass insertions which enter the dipole operator coefficients, $C_G^{ds\pm}$. Constraints on the chiral structure of the $\Delta I = \frac{1}{2}$ Lagrangian pointed out in the previous section require $|\delta\tilde{m}_{d_L s_R}^2| \gtrsim (2 - 4) |\delta\tilde{m}_{d_R s_L}^2|$ for large dipole-induced contributions. This suggests that the $\delta\tilde{m}_{d_L s_R}^4$ term in eq. (B1) is the most important for constraining the magnitude of the induced $\Delta I = \frac{1}{2}$ amplitude. The sign of its contribution to Δm_K is the same as the standard model contribution and the observed mass difference. However, both the $\delta\tilde{m}_{d_L s_L}^2 \delta\tilde{m}_{d_R s_R}^2$ and $\delta\tilde{m}_{d_L s_R}^2 \delta\tilde{m}_{d_R s_L}^2$ terms can have opposite sign and can compensate.¹⁷

In order to study the relative importance of the first three terms in eq. (B1) we equate, separately, the magnitudes of the first and third terms to Δm_K^{exp} and plot the corresponding upper bounds on $\delta\tilde{m}_{d_L s_R}^4/m_{\tilde{q}}^6$ and $\delta\tilde{m}_{d_L s_R}^2 \delta\tilde{m}_{d_R s_L}^2/m_{\tilde{q}}^6$, respectively, in Fig. 6 as a function of x .¹⁸ For $x \sim .01$ to 1 (corresponding to weak scale gluinos and weak to TeV scale squarks) and dominance of Q_G^{ds+} , Fig. 6 confirms that the first term in eq. (B1) provides the most important constraint on the induced $\Delta I = \frac{1}{2}$ amplitude. Its contribution to Δm_K would be considerably larger than that of the next two terms. However, for $x \lesssim .01$ substantial cancellations are possible between the first two terms and the third term.

In Fig. 7a we plot upper bounds from Δm_K on the contribution of Q_G^{ds+} to R_0 , the ratio of the induced $\Delta I = \frac{1}{2}$ amplitude to the observed amplitude, for weak scale gluino masses. The bounds correspond to setting the first term in eq. (B1) to Δm_K^{exp} , $2\Delta m_K^{exp}$ and $3\Delta m_K^{exp}$. The more liberal bounds take into account the possibility of accidental cancellations, up to 1 part in 3 - 4, among the supersymmetric contributions to Δm_K . C_G^{ds+} is evolved from $m_{\tilde{q}}$ to $m_c = 1.4 GeV$ taking all relevant thresholds, including $m_{\tilde{g}}$, into account.

According to Fig. 7a the induced $\Delta I = \frac{1}{2}$ amplitude can account for 30% to 50% of the observed amplitude if the unknown suppression factor m_K^2/Λ^2 lies in the range .2 to .4, as suggested in the model-independent analysis. This is especially true for lighter gluino masses or for small x because the loop integral $E(x)$, associated with the larger of the two contributions in eq. (60), gluon emission from the gluino line, increases substantially as x decreases. Note that an accelerator lower limit on the gluino mass is difficult to obtain since gluino cascade decay depends on many

¹⁷Note that the integrals $f_6(x)$ and $\tilde{f}_6(x)$ have opposite sign, while the various squark mass insertions can either be positive or negative.

¹⁸Since gluino and squark masses are not fixed by x we take $\alpha_s = .11$ in obtaining Fig. 6, which is a reasonable approximation for weak or TeV scale squarks.

parameters. Although a strict lower limit is close to 95 GeV , it is more likely to be around 125 GeV [55].

In Fig. 7b we plot upper bounds on the mass parameter

$$\tilde{m}_{d_L s_R} \equiv \frac{\delta \tilde{m}_{d_L s_R}^2}{m_{\tilde{q}}}, \quad (61)$$

corresponding to the bounds in Fig. 7a. $\tilde{m}_{d_L s_R}$ essentially measures the amount of $SU(2)_L$ breaking contained in $\delta \tilde{m}_{d_L s_R}^2$. It should not be much larger than the weak scale, based on the requirement that massive Higgs-squark scalar trilinear coupling coefficients should be less than or of order the squark mass scale in order to prevent $SU(3)_C$ breaking [47]. From Fig. 7b it follows that, for the gluino masses we've chosen, the squark masses can not be much larger than 2 or 3 TeV when saturating the Δm_K bounds. According to Fig. 7a this is not very restrictive as far as $\Delta I = \frac{1}{2}$ enhancement is concerned. Note that Fig. 7b confirms the validity of the squark mass insertion approximation in the region of squark masses of interest.

In Fig. 7c we study implications of $\Delta I = \frac{1}{2}$ enhancement for the quark mass spectrum. Upper bounds on the induced quark mass $\Delta m_{ds}^+(m_c)$, corresponding to the bounds of Fig. 7a, are plotted in order to probe dependence on the gluino and squark masses. According to Figs. 7a and 7c generation of θ_c or m_s (corresponding to $\Delta m_{ds}^+ \sim 35 \text{ MeV}$) together with a large dipole-induced $\Delta I = \frac{1}{2}$ amplitude favors lighter gluino masses, $m_{\tilde{g}} \sim 125 \text{ GeV}$ to 175 GeV , and lighter squark masses, $m_{\tilde{q}} \sim \frac{1}{2} \text{ TeV}$. Note that $m_{\tilde{q}}$ in this range corresponds to *Region II* of our model-independent analysis.¹⁹

To make further contact with the model-independent analysis we plot contours of constant R_0 in the $(|\xi_{ds}^+|, m_{\tilde{q}})$ plane of Fig. 8. Contours of constant Δm_K , again corresponding to contributions of the first term in eq. (B1), are also included in order to determine the allowed regions of the plane. $m_{\tilde{q}} = 150 \text{ GeV}$ is chosen for illustrative purposes, reflecting the tendency towards larger $\Delta I = \frac{1}{2}$ amplitudes at lower gluino masses. $\text{BR}_\ell(B)$ contours are included for later comparison.

The similarities between Fig. 8 and Fig. 4 demonstrate that supersymmetry can provide a realization of our model-independent conclusions. In particular, we see that in Region II the induced $\Delta I = \frac{1}{2}$ amplitude can reasonably account for $75 \frac{m_K^2}{\Lambda^2} \%$

¹⁹Given $\Delta m_{ds}^+ \sim \theta_c m_s$, generation of θ_c would correspond to $\delta \tilde{m}_{1L2R}^2 \sim \delta \tilde{m}_{d_L s_R}^2$ while generation of m_s would correspond to $\delta \tilde{m}_{2L2R}^2 \sim \frac{\delta \tilde{m}_{d_L s_R}^2}{\theta_c}$. According to Fig. 7b, $\frac{\delta \tilde{m}_{1L2R}^2}{m_{\tilde{q}}}$ and $\frac{\delta \tilde{m}_{2L2R}^2}{m_{\tilde{q}}}$ would be sufficiently small in each case when compared to the weak scale.

to $150\frac{m_K^2}{\Lambda^2}$ % of the observed amplitude, in direct association with generation of θ_c or m_s ($\xi_{ds}^+ \sim 1$). However, the larger $\Delta I = \frac{1}{2}$ amplitudes may require a one part in 3 - 4 cancelation among the supersymmetric contributions to Δm_K . Again, we remind the reader that our estimates of the latter are fairly crude, especially since the vacuum saturation approximation has been used. Alternatively, for larger squark masses $\Delta I = \frac{1}{2}$ enhancement will require a small tuning of θ_c or m_s . Finally, we have not taken into account the potential contribution of Q_G^{ds-} to the $\Delta I = \frac{1}{2}$ amplitude. As previously noted, $K \rightarrow 3\pi$ constraints probably allow $\mathcal{O}(10\%)$ of the observed amplitude to come from this source. Associated contributions to Δm_K from the second and third terms in eq. (B1) would be sufficiently small. The amplitudes generated by Q_G^{ds-} and Q_G^{ds+} can, a priori, add constructively, strengthening our conclusion that the chromomagnetic dipole moments could account for 30% to 50% of the observed $\Delta I = \frac{1}{2}$ amplitude.

Ultra-light Gluinos

Finally, we consider $\Delta I = \frac{1}{2}$ enhancement for gluinos in the ‘light-gluino window’ [56, 27, 57, 58], corresponding to $m_{\tilde{g}} \sim 1$ to 4 GeV , or $x \lesssim 10^{-3}$ for weak scale or heavier squarks. Here we are motivated by the observation that the allowed dipole-induced $\Delta I = \frac{1}{2}$ amplitude increases with decreasing x . It has been claimed that light gluinos would also lead to better agreement between the LEP measurement of $\alpha_s(M_Z)$ and determinations of α_s at lower energies [57, 58] since they would slow the running of α_s below M_Z . Whether there really is a discrepancy between the proper extraction of α_s from LEP and other experiments, or whether parts of the light-gluino window are actually not ruled out [59] are issues which have become increasingly controversial of late about which we have nothing further to add.

In Figs. 9a, 9b and 9c we plot upper bounds on R_0 , $\tilde{m}_{d_L s_R}$ and $\Delta m_{ds}^+(m_c)$, respectively, obtained as usual from contributions of the first term in eq. (B1) to Δm_K . Following ref. [58], we choose $\alpha_s(M_Z) = .124$, and evolve downwards at two-loops taking into account all relevant thresholds. We see that for squarks in the 200 GeV to 400 GeV range, $R_0 \sim \frac{m_K^2}{\Lambda^2}$ to $2\frac{m_K^2}{\Lambda^2}$ can be obtained with little or no tuning of Δm_K , whereas $R_0 \sim 3\frac{m_K^2}{\Lambda^2}$ may require a moderate one part in three to four tuning. So for ultra-light gluinos, Q_G^{ds+} could account for at least half of the observed $\Delta I = \frac{1}{2}$ amplitude. However, according to Fig. 6, a hierarchy of $\mathcal{O}(30)$ between $\delta\tilde{m}_{d_L s_R}^2$ and $\delta\tilde{m}_{d_R s_L}^2$ would be required in order to satisfy Δm_K constraints. This condition is discussed further in Appendix A.

The radiatively induced quark masses are generally too small to be relevant, with $\Delta m_{ds}^+ \sim 1 \text{ MeV}$ to 10 MeV typical. A possible exception arises for squarks near the TeV scale. For example, $\Delta m_{ds}^+(m_c) \sim \theta_c m_s$ can be obtained for $m_{\tilde{q}} \sim 800 \text{ GeV}$ and $m_{\tilde{g}} \sim 4 \text{ GeV}$. Unfortunately, according to Fig. 6, a very large hierarchy of $\mathcal{O}(300)$ would be required between $\delta\tilde{m}_{d_L s_R}^2$ and $\delta\tilde{m}_{d_R s_L}^2$, and $\tilde{m}_{d_L s_R}$ would have to lie in the 200 GeV to 300 GeV range, which is on the high end for an $SU(2)_L$ breaking squark mass. So although ultra-light gluinos are promising for $\Delta I = \frac{1}{2}$ enhancement, this case does not conform to the conclusions of our model-independent analysis regarding quark mass generation. Because of the extreme values of x , ζ_G is substantially larger than 1, contrary to what is naively expected, so that large $\Delta I = \frac{1}{2}$ enhancement is associated with relatively small induced quark masses.

Suppression of $\text{BR}_\ell(B)$ and Radiative B Decays.

Next we discuss supersymmetric generation of the chromomagnetic dipole operators $Q_G^{sb\pm}$ and $Q_G^{db\pm}$ via the b penguin analogs of Fig. 5. These diagrams have been studied extensively in the past [51]. We will see that they can resolve the discrepancy between the measured value of $\text{BR}_\ell(B)$ and the parton model prediction in the standard model and that this has rich implications for the quark mass spectrum and radiative B decays. Again we will consider both weak scale and ultra-light gluinos.

Expressions for the operator coefficients $C_G^{sb\pm}$, $C_G^{db\pm}$, and for the radiatively induced masses Δm_{sb}^\pm , Δm_{db}^\pm follow by analogy from eq. (60). $\Gamma(b \rightarrow sg)$ and $\Gamma(b \rightarrow dg)$ follow from eq. (28). The electromagnetic dipole operator coefficients are given by

$$C_F^{sb+}(m_{\tilde{q}}) = -\frac{2\alpha_s}{3\pi} \frac{x}{m_{\tilde{q}}} C(x) \frac{\delta\tilde{m}_{s_L b_R}^2}{m_{\tilde{q}}^2} \quad (62)$$

$$C_F^{sb-}(m_{\tilde{q}}) = -\frac{2\alpha_s}{3\pi} \frac{x}{m_{\tilde{q}}} C(x) \frac{\delta\tilde{m}_{s_R b_L}^2}{m_{\tilde{q}}^2}, \quad (63)$$

and similarly for the coefficients C_F^{db+} and C_F^{db-} . Expressions for $\Gamma(b \rightarrow s\gamma)$ and $\Gamma(b \rightarrow d\gamma)$ follow from eq. (39). Finally, the supersymmetric box graph contributions to $\Delta m_B \equiv m(B_d^0) - m(\overline{B}_d^0)$ are given in eq. (B2).

We are interested in suppression of $\text{BR}_\ell(B)$ due to the inclusive gluon channel decay width, as in the model-independent plots of Figs. 2 and 4. In Fig.10a we plot contours of constant $\text{BR}_\ell(B)$, for weak scale gluino masses, in the plane of $\Delta m'(m_c)$ vs. $m_{\tilde{q}}$ ($\Delta m'$ was defined in (31)). Although $\Delta m'$ is proportional to V_{cb} along these contours, this dependence and the accompanying uncertainty drop out for ξ' (defined in (32)). In Fig. 8 contours of $\text{BR}_\ell(B)$ have been included in the $(\xi', m_{\tilde{q}})$ plane for

$m_{\tilde{q}} = 150 \text{ GeV}$. According to Fig. 10a or Fig. 8, supersymmetry can provide a realization of the model-independent conclusions of Fig. 2:

- (i) In Region I, corresponding to $m_{\tilde{q}} \sim 1 \text{ TeV}$ to 2 TeV , the desired $\text{BR}_\ell(B)$ suppression is associated with $\xi' \sim 1$ for a wide range of gluino masses.
- (ii) In Region II, corresponding to $m_{\tilde{q}} \sim 300 \text{ GeV}$ to 700 GeV , $\text{BR}_\ell(B)$ suppression is associated with $\xi' \sim .1$ for gluino masses below 200 GeV .

Potential implications for the quark mass spectrum have been discussed in Section 3 and Appendix A. Restrictions special to the supersymmetric case are discussed below.

To check that the $SU(2)_L$ breaking squark mass insertions responsible for $\text{BR}_\ell(B)$ suppression are not too large we define the mass parameter

$$\tilde{m}' \equiv \frac{(\delta\tilde{m}_{s_L b_R}^2 + \delta\tilde{m}_{b_L s_R}^2 + \delta\tilde{m}_{d_L b_R}^2 + \delta\tilde{m}_{b_L d_R}^2)}{m_{\tilde{q}}}, \quad (64)$$

and plot contours of constant $\text{BR}_\ell(B)$ in the $(\tilde{m}', m_{\tilde{q}})$ plane of Fig. 10b. We also include upper bounds on $\tilde{m}_{d_L b_R}$, obtained by setting the analog of the first term in eq. (B1) equal to $m(B_d^0) - m(\overline{B}_d^0)$. Comparison of Figs. 10a and 10b confirms that $B_d^0 - \overline{B}_d^0$ mixing does not significantly constrain $\text{BR}_\ell(B)$ suppression. However, limitations on the size of $SU(2)_L$ breaking squark mass insertions determine which features of the quark mass spectrum can be accounted for. In particular, in Region I, $\xi' \sim 1$ can be associated with generation of V_{cb} but not with the alternative, generation of m_b . In Region II, $\xi' \sim .1$ can be associated with generation of V_{ub} but not with the alternative, simultaneous generation of V_{cb} and m_b .²⁰

In Region II large hierarchies are not required among the left-right down squark mass insertions²¹. Equivalently, all entries of the radiatively induced quark mass matrix, Δm_{ij} , can be of order $\theta_c m_s$ or $V_{ub} m_b$, thereby accounting for θ_c , V_{ub} , and m_d .

To study implications for radiative B decays, contours of constant $\text{BR}_\ell(B)$ are drawn in the plane of $\text{BR}(b \rightarrow x\gamma)$ vs. $m_{\tilde{q}}$. These contours are essentially independent of V_{cb} . Only the supersymmetric contributions to $b \rightarrow x\gamma$ are taken into account but, a priori, the standard model contributions could add constructively or destructively.

²⁰According to Fig. 10b, in the ruled out scenarios $\delta\tilde{m}_{3_L 3_R}^2/m_{\tilde{q}}$ would be much larger than the weak scale.

²¹ $\frac{\delta\tilde{m}_{i_L j_R}^2}{m_{\tilde{q}}}$ can be of order a few GeV for all i,j.

According to Fig. 10c, the following can be concluded:

- In Region I, with $\xi' \sim 1$, new contributions to $\text{BR}(b \rightarrow s\gamma)$ tend to lie below the standard model contribution, $(2 - 3) \times 10^{-4}$, unless the gluinos are heavy. Eq. (33) implies that contributions to $\text{BR}(b \rightarrow d\gamma)$ will be two orders of magnitude smaller, as in the standard model.
- In Region II, with $\xi' \sim .1$, new contributions to $\text{BR}(b \rightarrow x\gamma)$ are $\mathcal{O}(10^{-4})$. If $\Delta m_{db}^+ \sim V_{ub}m_b$, as in eq. (34), and as suggested by the quark mass spectrum, then $\text{BR}(b \rightarrow d\gamma) \sim (.1 - 1) \times 10^{-4}$, a dramatic departure from the standard model.

Ultra-light Gluinos

As in the case of $\Delta I = \frac{1}{2}$ enhancement we end discussion of $\text{BR}_\ell(B)$ suppression with the case of gluinos in the ‘light-gluino’ window. Figs. 11a,b are the analogs of Figs. 10a,b, respectively, for $m_{\tilde{g}} = 1 \text{ GeV}$ and 4 GeV . $\text{BR}_\ell(B) \sim 10\% - 11\%$ is readily obtained, and $B_d^0 - \bar{B}_d^0$ mixing and $SU(2)_L$ breaking constraints on the squark mass insertions are easily satisfied. However, as for $\Delta I = \frac{1}{2}$ enhancement with light gluinos, the quark mass contributions do not play a significant role except perhaps for squark masses in the 800 GeV to 1 TeV region. In this case $\Delta m_{db}^+ \sim 20 \text{ MeV}$, or $\mathcal{O}(V_{ub}m_b)$, could help account for V_{ub} . Finally, new contributions to $\text{BR}(b \rightarrow x\gamma)$ depend weakly on $m_{\tilde{q}}$ and are $\mathcal{O}(2 - 3) \times 10^{-5}$. All left-right squark mass insertions can be of same order since the radiative quark mass contributions are small, implying that $\text{BR}(b \rightarrow d\gamma)$ can be an order of magnitude larger than in the standard model.

To summarize, comparison of Figs. 4 and 8 reveals that *Region I* or *Region II* dipole-operator phenomenology can be realized in supersymmetric models with weak scale gluinos. In particular, it is possible to tie in $\text{BR}_\ell(B)$ suppression with radiative generation of V_{ub} (Region II) or V_{cb} (Region I). It should also be possible to tie in 30% - 50% of the $\Delta I = \frac{1}{2}$ amplitude with radiative generation of θ_c or m_s (Region II). For larger squark masses the Δm_K constraints are weaker, but a small tuning of θ_c or m_s would be required. For ultra-light gluinos, $\text{BR}_\ell(B)$ suppression and larger $\Delta I = \frac{1}{2}$ amplitudes are possible, but it is difficult to relate these effects to the quark mass spectrum. Finally, $\text{BR}_\ell(B)$ suppression in Region II is associated with large contributions to $\text{BR}(b \rightarrow d\gamma)$, lying in the range $(.1 - 1) \times 10^{-4}$. For ultra-light gluinos, contributions of order $(1 - 3) \times 10^{-5}$ are possible.

Supersymmetric models of chromomagnetic dipole operator phenomenology face

difficulties in supergravity theories with general Kähler potential, or in string theories with moduli-driven supersymmetry breaking [60].²² In particular, the expected magnitudes [62, 48] of off-diagonal left-right squark mass insertions will be too small to accommodate Region I phenomenology, and will rule out any chance for a connection to the quark spectrum with ultra-light gluinos. Those mass insertions which involve the 3rd generation, $\delta\tilde{m}_{1L3R}^2$, $\delta\tilde{m}_{2L3R}^2$, etc., are expected to be $\mathcal{O}(m_{susy}m_b)$, which is large enough to obtain $\text{BR}_\ell(B)$ suppression and V_{ub} in Region II, or $\text{BR}_\ell(B)$ suppression with ultra-light gluinos. Finally, the left-right squark mass insertions of relevance to the $\Delta I = \frac{1}{2}$ amplitude are expected to be $\mathcal{O}(m_{susy}m_s)$ which is about an order of magnitude smaller than required for significant enhancement with weak-scale or ultra-light gluinos. However, these estimates of the mass insertions are uncertain by at least a factor of 3, since there are many dimensionless parameters in the Kähler potential which could be $\mathcal{O}(1)$. Larger contributions to these mass insertions may also arise if ‘hidden sector’, or string-moduli fields couple to the observable sector via non-renormalizable terms.[63]

It is suggestive that in supersymmetric models radiative mass contributions associated with $\text{BR}_\ell(B)$ suppression or $\Delta I = \frac{1}{2}$ enhancement are often of the right magnitude to account for several features of the quark mass spectrum. However, it remains to construct supersymmetric models in which they provide a unique origin for these features. In particular, one would have to show that supersymmetry breaking can lead to large enough flavor symmetry breaking in the squark sector in models in which tree-level Higgs Yukawa couplings are not important for the light quark spectrum.

In contrast, the dipole operators are often a necessary outcome of quark mass generation in technicolor models, or in models of quark and lepton substructure. Next, we discuss a class of technicolor models with large chromomagnetic dipole moments.

5. Techniscalar Models

We begin with a brief description of techniscalar models [64]. Unlike in extended technicolor (ETC) models [65], the technicolor gauge group is not extended to a horizontal group. Instead, the ETC gauge bosons are replaced with technicolored

²²Supergravity theories with minimal Kähler potential, or string theory scenarios with dilaton driven [60, 61] supersymmetry breaking can not generate large enough dipole operator coefficients.

scalars (techniscalars). Flavor-changing neutral currents first arise at the one-loop level and are suppressed. Furthermore, the quark-techniscalar- technifermion Yukawa couplings can vary substantially. These features allow the masses of all techniscalars to be of order 1 TeV . In contrast, $\mathcal{O}(100 \text{ TeV})$ masses are required for ETC gauge bosons which couple to the light quarks.

Consider the gauge group $G = SU(N)_{TC} \times SU(3)_C \times SU(2)_L \times U(1)_Y$, together with three quark families and the following technicolored fields: a right-handed $SU(2)_L$ doublet of technifermions $T_R(N, 1, 2, 0) = (U_R, D_R)^T$, two left-handed $SU(2)_L$ singlet technifermions $U_L(N, 1, 1, 1/2)$, $D_L(N, 1, 1, -1/2)$, all with charges $\pm\frac{1}{2}$, and a charge $\frac{1}{6}$ techniscalar $\omega(\overline{N}, 3, 1, 1/6)$. Transformation properties with respect to the technicolor group, $SU(N)_{TC}$, and the standard model gauge group have been included in parenthesis. The most general quark Yukawa couplings are given by

$$\mathcal{L}_Y = \mathbf{h}_i \omega \overline{Q}_L^i T_R + \mathbf{h}_i^{u\dagger} \omega^* \overline{U}_L u_R^i + \mathbf{h}_i^{d\dagger} \omega^* \overline{D}_L d_R^i + H.c., \quad (65)$$

where \mathbf{h}^u , \mathbf{h}^d and \mathbf{h} are dimensionless three-component Yukawa coupling vectors and latin indices label the quark interaction basis states. ω acquires an explicit mass from the scalar sector of the Lagrangian and a ‘constituent’ mass from technicolor dynamics.²³ As usual we ignore CP violation and take all parameters to be real.

Technifermion condensates will induce up and down quark mass matrices via techniscalar exchange. In the limit $m_\omega \gg \Lambda_{TC}$, where $\Lambda_{TC} \sim 1 \text{ TeV}$, the down mass matrix, in the interaction basis, is given by

$$\Delta m_{ij} \approx \mathbf{h}_i \mathbf{h}_j^{d\dagger} \frac{\langle \overline{D} D \rangle}{4m_\omega^2}. \quad (66)$$

The up quark matrix is analogous. The technifermion condensates are estimated to be [39]

$$\langle \overline{D} D \rangle = \langle \overline{U} U \rangle \sim \left(\frac{3}{N_{TC}} \right)^{\frac{1}{2}} 4\pi \left(\frac{v}{\sqrt{N_D}} \right)^3 \text{ GeV}^3, \quad (67)$$

where $v = 246 \text{ GeV}$, and N_D (equal to 1 above) is the number of technifermion doublets.

²³ Scalar technicolor models can be supersymmetrized in order to protect the masses of the scalars. In turn, supersymmetric FCNC can be suppressed since a multi-TeV supersymmetry breaking scale is natural in this framework [66].

Chromomagnetic dipole operators are due to emission of a gluon by the exchanged techniscalar. The down quark coefficients are given by

$$C_G^{ij} \approx \frac{\Delta m_{ij}}{2m_\omega^2} \quad (68)$$

at m_ω . Note that C_G and Δm are proportional, rank 1 matrices. In terms of the general parametrization in (24), the above example corresponds to $\zeta_G \approx \frac{1}{2}$. To estimate the physical (flavor-changing) chromomagnetic dipole moments we insert this value into the model-independent expressions in (26),(27) for $C_G^{ds\pm}$, $C_G^{sb\pm}$, and $C_G^{db\pm}$, and identify the scale of new physics M with m_ω . The renormalization scale factor $\eta(\mu)$ is the same as in eq. (24) for non-supersymmetric models.

We will mainly be interested in the case $m_\omega \sim \Lambda_{TC}$, especially for m_ω in Region II. Unfortunately, it is difficult to calculate the induced quark masses and dipole moments in this case since strong technicolor dynamics become important. For example, it may be that the exchanged techniscalar and technifermion bind so that the quark's mass can be interpreted as due to mixing with a composite heavy quark. Nevertheless, we expect the above expressions to give the correct orders of magnitude, and we still expect proportionality between Δm and C_G .

In models with a minimal set of technifermions and a single techniscalar only a single family acquires masses from techniscalar exchange, which we identify with m_t and m_b .²⁴ Note that $SU(2)_L$ invariance automatically aligns the left-handed top and bottom mass eigenstates (at 0'th order in light quark masses), as required by the KM hierarchy. Exchange of an additional techniscalar (copy of ω) or an additional set of technifermions (copies of T_R , U_L , D_L) with smaller Yukawa couplings can generate a second unit-rank matrix for up quarks and for down quarks, with eigenvalues of order m_c and m_s , respectively. This time $SU(2)_L$ invariance insures approximate alignment of the left-handed charm and strange eigenstates, as required by θ_c . (Some details of these models are discussed in Appendix A.) First generation masses, θ_c and V_{ub} could also be due to techniscalar exchange or they could have an entirely different origin. For example, additional supersymmetric or multi-scalar flavor physics could generate radiative mass contributions of $\mathcal{O}(\theta_c m_s)$, as we saw in the previous section. Alternatively, Higgs doublets can obtain small vacuum expectation values by coupling to the technifermions[67, 66]. If they are very heavy and, or, their couplings are small they could simultaneously account for the light quark spectrum and evade

²⁴One obtains $m_t \approx |\mathbf{h}| |\mathbf{h}^u| \langle \bar{U}U \rangle / 4m_\omega^2$, and $m_b \approx |\mathbf{h}| |\mathbf{h}^d| \langle \bar{D}D \rangle / 4m_\omega^2$.

FCNC bounds.²⁵

We begin with a phenomenological analysis of $\Delta I = \frac{1}{2}$ enhancement and $\text{BR}_\ell(B)$ suppression due to exchange of a single techniscalar-technifermion pair, leading to the masses and chromomagnetic operator coefficients of eqs. (66), (68). From this analysis we hope to learn which features of the quark mass spectrum, or which scenarios outlined above, are most naturally associated with either phenomenon.

$\Delta I = \frac{1}{2}$ enhancement, $\text{BR}_\ell(B)$, and radiative B decays

In Fig. 12a contours of constant $\Delta I = \frac{1}{2}$ enhancement, or R_0 , in the plane of $|\xi_{ds}^+ - \xi_{ds}^-|$ vs. m_ω are obtained by taking $\zeta_G \approx \frac{1}{2}$ in the analysis leading to Fig. 4. It should come as no surprise that $\Delta m_{ds}^+ \sim 30 - 50 \text{ MeV}$, or $\xi_{ds}^+ \sim 1$, singles out *Region II* for substantial $\Delta I = \frac{1}{2}$ enhancement, corresponding to $R_0 \sim (1 - 1.5) \frac{m_K^2}{\Lambda^2}$. An important question is whether technicolor dynamics allow m_ω in Region II? Estimates of the technifermion constituent mass [68] (obtained by scaling the QCD constituent mass) give

$$m_{TC} \sim (300 \text{ MeV}) \frac{v}{\sqrt{N_D} f_\pi}, \quad (69)$$

or 800 GeV for $N_D = 1$, 550 GeV for $N_D = 2$. Assuming that techniscalar ‘constituent’ masses are of same order we take as a reasonable bound $m_\omega \gtrsim \frac{1}{2} \text{ TeV}$ which of course would allow for solutions in Region II.

To examine the relevance, or lack thereof, of Δm_K constraints it is necessary to define the Yukawa couplings of the left-handed and right-handed quark mass eigenstates to ω :

$$\lambda_q \equiv \langle q_L | \mathbf{h} \rangle, \quad \bar{\lambda}_q \equiv \langle \mathbf{h}^d | q_R \rangle, \quad q = d, s, b. \quad (70)$$

The quark masses Δm_{ds}^+ and Δm_{ds}^- are proportional to $\lambda_d \bar{\lambda}_s$ and $\lambda_s^* \bar{\lambda}_d^*$, respectively. To get rough estimates of new box-graph contributions to Δm_K in terms of these couplings we ignore technicolor interactions and assign the technifermions in the loops a mass equal to the technifermion ‘constituent mass’, m_{TC} , in eq. (69). The resulting expressions are given in eq. (B2) of Appendix B. In Fig. 12b we plot contours of R_0 in the plane of $|\lambda_d \bar{\lambda}_s - \bar{\lambda}_d \lambda_s|$ vs. m_ω , for $N_{TC} = 4$ and $N_D = 1$. We also include an ‘upper-bound’ on $\lambda_d \bar{\lambda}_s$, obtained by setting the first term in eq. (B2) equal to Δm_K^{exp} .

²⁵ However, this option does not have a built-in mechanism for alignment of charm and strange eigenstates.

Remarkably, and in spite of the crude nature of our estimates, this result clearly indicates that Δm_K constraints are not a factor in limiting $\Delta I = \frac{1}{2}$ enhancement in techniscalar models, unlike what we saw in supersymmetric models.²⁶ The remaining terms in eq. (B2) are also not restrictive. In fact, the main constraint on $\Delta I = \frac{1}{2}$ enhancement comes from θ_c or m_s .

For $\text{BR}_\ell(B)$ suppression we are, as usual, interested in the cumulative effects of $Q_G^{ds\pm}$ and $Q_G^{db\pm}$. Contours of $\text{BR}_\ell(B) = 10\%, 11\%$ in the $(|\xi'|, m_\omega)$ plane can be read off directly from the model-independent plots of Figs. 2 or 4 by taking $\zeta_G \approx \frac{1}{2}$, and are included in Fig. 12a. As expected, $\xi' \sim 1$ singles out Region I ($m_\omega \sim 1 - 1.5 \text{ TeV}$) for $\text{BR}_\ell(B)$ suppression, while $\xi' \sim .1$ singles out Region II ($m_\omega \sim \frac{1}{2} \text{ TeV}$).

What about radiative b decays in these models? The electromagnetic dipole operators $Q_F^{sb\pm}$ and $Q_F^{db\pm}$ are induced by radiation of a photon from the exchanged techniscalar. Similar contributions have been considered in extended technicolor models [69]. The operator coefficients $C_F^{sb\pm}$ and $C_F^{db\pm}$ are given at m_ω by

$$C_F^{sb\pm} \approx \frac{Q_\omega}{Q_d} \frac{\Delta m_{sb}^\pm}{2m_\omega^2}, \quad C_F^{db\pm} \approx \frac{Q_\omega}{Q_d} \frac{\Delta m_{db}^\pm}{2m_\omega^2}. \quad (71)$$

Comparison with the model-independent parametrization of Section 3, eqs. (27), (38), gives $\frac{\zeta_F}{\zeta_G} = \frac{Q_\omega}{Q_d} = -\frac{1}{2}$. According to Fig. 3, new contributions to $\text{BR}(b \rightarrow x\gamma)$ associated with $\text{BR}_\ell(B)$ suppression must therefore lie below the CLEO bound. This is borne out in Fig. 12c. In both Region I and Region II one obtains $\text{BR}(b \rightarrow x\gamma) \sim (2 - 3) \times 10^{-4}$. Given $\Delta m_{db}^\pm \sim V_{ub} m_b$, we expect $\text{BR}(b \rightarrow d\gamma) \sim 10^{-2} \cdot \text{BR}(b \rightarrow s\gamma)$ in Region I, but in Region II, as usual, $\text{BR}(b \rightarrow d\gamma)$ is likely to exceed the standard model prediction by an order of magnitude or more. Finally, we mention that new contributions to $B^0 - \overline{B}^0$ mixing are too small to constrain $\text{BR}_\ell(B)$ suppression, as one would expect from the weakness of Δm_K constraints.

Implications of Quark Mass Generation

Implications of quark mass generation for $\Delta I = \frac{1}{2}$ enhancement and $\text{BR}_\ell(B)$ suppression are summarised below. Details are provided in Appendix A. We assume that m_t and m_b are due to techniscalar exchange, and that an interaction basis exists in which the full down quark mass matrix respects the hierarchy of eq. (A1):

(a) If only 3rd generation masses are due to techniscalar exchange (minimal techniscalar model) we expect $\Delta m_{sb}^\pm \sim V_{cb} m_b$ and $\Delta m_{db}^\pm \sim V_{ub} m_b$, or $\xi' \sim 1$. This means

²⁶ Δm_K constraints for $N_D = 2$ are slightly more restrictive, but our conclusions would not change qualitatively.

that $\text{BR}_\ell(B)$ suppression must take place in Region I. However, Δm_{ds}^\pm would be too small to obtain substantial $\Delta I = \frac{1}{2}$ enhancement.

(b) If a second set of technifermions is introduced ($N_D = 2$) in order to generate m_c , m_s and V_{cb} then $\Delta I = \frac{1}{2}$ enhancement and $\text{BR}_\ell(B)$ suppression are naturally accommodated in *Region II*. The reason is that C_G and Δm remain proportional even though they are now of rank 2. This means that Δm_{sb}^+ and Δm_{sb}^- will be $\mathcal{O}(V_{ub}m_b)$ or $\mathcal{O}(\theta_c m_s)$, since they will be determined by mass contributions responsible for first generation masses and mixing angles. Δm_{ds}^\pm and Δm_{db}^\pm will also be of this order, implying that $\xi' \sim .1$ and $\xi_{ds}^\pm \sim 1$, so Region II phenomenology is singled out. In particular, 30% – 50% of the $\Delta I = \frac{1}{2}$ amplitude may be attributable to $Q_G^{ds\pm}$.²⁷ In general, there will be deviations from proportionality of C_G and Δm due to non-universal technifermion current mass²⁸ corrections or radiative Yukawa coupling corrections to the technifermion propagators. However, the propagators are dominated by large and universal constituent masses, so these corrections are generally too small to alter our conclusions significantly.²⁹

(c) If 2nd generation masses and V_{cb} are due to a second techniscalar, $\text{BR}_\ell(B)$ suppression again singles out Region I, as in (a). Only in the limit of degenerate or nearly degenerate techniscalar masses are $\Delta I = \frac{1}{2}$ enhancement and $\text{BR}_\ell(B)$ suppression possible in Region II, since C_G and Δm would be nearly proportional, as in (b). However, in the absence of additional (horizontal) symmetries an order of magnitude tuning of techniscalar masses would be required.

(d) Finally, if 1st generation masses and mixing angles are due to exchange of a second (if there are already two sets of technifermions responsible for 2nd and 3rd generation masses) or third techniscalar, then they can be associated with Region

²⁷As an illustrative example, consider $\frac{m_K^2}{\Lambda^2} \approx .2$ and $m_\omega \approx \frac{1}{2} \text{ TeV}$. According to Fig. 12a, $\xi_{ds}^+ \sim 1$ and $\xi_{ds}^- \sim -.5$ would generate 30% of the $\Delta I = \frac{1}{2}$ amplitude. Only 10% would be due to Q_G^{ds-} , so constraints on the chiral structure of the $\Delta I = \frac{1}{2}$ Lagrangian would be satisfied. If we further allow $\xi_{ds}^+ \approx 1.5$ (which requires less than a 1 part in 2 tuning between different contributions to m_s), or $m_K^2/\Lambda^2 \approx .3$, then 50% of the $\Delta I = \frac{1}{2}$ amplitude would be accounted for.

²⁸Technifermion current masses insure sufficiently heavy technipions. One possibility for their origin is exchange of heavy gauge-singlet scalars, leading to effective four-technifermion operators.

²⁹One might expect corrections to $C_G^{sb\pm}$ are $\mathcal{O}(\frac{\delta m}{m_{TC}} \frac{m_b V_{cb}}{m_\omega^2})$, where $m_{TC} \sim m_\omega \sim \frac{1}{2} \text{ TeV}$ and δm is a typical technifermion current mass. For example, $\delta m \sim 10 - 50 \text{ GeV}$ would produce $\mathcal{O}(\frac{200}{\sqrt{N_D}} - \frac{450}{\sqrt{N_D}} \text{ GeV})$ technipion masses, but corrections to $C_G^{sb\pm}$ would be $\lesssim \frac{(20 \text{ MeV})}{m_\omega^2}$ for $N_D = 2$.

II phenomenology.³⁰ If first generation masses and mixing angles are not due to techniscalar interactions they might still be associated with contributions to Region II phenomenology, as we saw in the previous two sections.

In techniscalar models the connection between the quark spectrum and dipole operator phenomenology is transparent, and the potentially rich phenomenological implications of new flavor physics, particularly in Region II, are well-illustrated. Yet a further consequence of a light $\frac{1}{2} TeV$ techniscalar would be a large top chromomagnetic dipole moment, leading to substantial enhancement of the Tevatron $t\bar{t}$ production cross-section [70]. This is relevant in light of recent evidence for top production at CDF [71].

It stands to reason that important operators of different dimension than the dipole moment operators may be generated by new flavor physics. We end this section with discussion of dimension-6 operators which impact on the decays $Z \rightarrow b\bar{b}$ and $b \rightarrow s\mu^+\mu^-$. In particular, we remark on the effects of the following interaction between quark and technifermion $SU(2)_L$ doublets,

$$\Delta\mathcal{L}_6 \approx -\frac{\mathbf{h}_i\mathbf{h}_j^\dagger}{4m_\omega^2}(\overline{Q_{L_i}}\gamma^\mu\tau^a Q_{L_j})(\overline{T_R}\gamma_\mu\tau^a T_R), \quad (72)$$

which is induced by techniscalar exchange. The effects of similar dimension-6 operators have been considered in ETC models [72, 69, 73, 74, 75].

For simplicity, we assume a minimal techniscalar scenario, as in (a) above. Replacing the technifermion current in (72) by a sigma-model current, as in [72, 76], and assuming the hierarchy in (A1), one obtains the following bottom quark couplings to the Z ,

$$\Delta\mathcal{L}_Z \approx \frac{m_t}{8\pi v} \left| \frac{\lambda_t}{\bar{\lambda}_t} \right| \frac{e}{\sin\theta\cos\theta} (\overline{b_L}\gamma^\mu b_L + \mathcal{O}(V_{cb})\overline{s_L}\gamma^\mu b_L + \mathcal{O}(V_{ub})\overline{d_L}\gamma^\mu b_L) Z_\mu. \quad (73)$$

Note that the $Zb_L b_L$ and $Zt_L t_L$ couplings increase in magnitude³¹, opposite to what happens in ordinary ETC models [72]. This is because the technifermion current in eq. (72) is right-handed, giving opposite sign axial-vector couplings. This is also the case in modified ETC models in which ETC gauge bosons carry $SU(2)$ charge [75].

³⁰However, if both 1st and 2nd generation masses are due to exchange of the same techniscalar, but different technifermions, C_G^{ds+} is suppressed and large $\Delta I = \frac{1}{2}$ amplitudes are not possible.

³¹By an amount $\frac{m_t}{8\pi v} \left| \frac{\lambda_t}{\bar{\lambda}_t} \right| \frac{e}{s_\theta c_\theta}$.

The resulting increase in $R_b \equiv \Gamma_b/\Gamma_h$, for $m_t \approx 170 \text{ GeV}$, relative to the standard model prediction of $\approx .216$, is estimated to be

$$\frac{\delta R_b}{R_b} \approx 9.9\% \left| \frac{\lambda_t}{\bar{\lambda}_t} \right| \left[\frac{m_t}{170 \text{ GeV}} \right]. \quad (74)$$

The LEP full fit [77], $R_b = 0.2202 \pm .0020$, corresponds to $\frac{\delta R_b}{R_b} < 2.9\%(1\sigma), 3.8\%(2\sigma)$, so we require $\frac{\lambda_t}{\bar{\lambda}_t} \sim \frac{1}{3}$. Adapting the ETC analysis of $b \rightarrow s\mu^+\mu^-$ in ref. [74] to the techniscalar case, we find

$$\text{BR}(b \rightarrow s\mu^+\mu^-) \approx 9 \times 10^{-5} \left(\frac{\lambda_t}{\bar{\lambda}_t} \right)^2, \quad (75)$$

or $\sim 10^{-5}$. This should be compared to the present upper bound [78] of 5×10^{-5} , and the standard model prediction [79] of $\approx 6 \times 10^{-6}$ for $m_t \approx 170 \text{ GeV}$. It is important to note that, quite generally, new contributions to R_b and $b \rightarrow s\mu^+\mu^-$ will be correlated as above.

6. Conclusion

We begin with a brief discussion of some of the relevant issues which have not been addressed in this paper. The first concerns CP violation in the Kaon system. Although we have set all CP violating phases to zero, chromomagnetic dipole operators can, in general, make substantial contributions to ϵ'/ϵ . In particular, if they account for 30% – 50% of the $\Delta I = \frac{1}{2}$ amplitude then the phases entering the dipole operator coefficients must be extremely small, satisfying

$$\left| \text{Arg}[C_G^{ds+} - C_G^{ds-}] \right| \leq (3 - 5) \times 10^{-4} \left| \frac{\epsilon'/\epsilon}{2 \times 10^{-4}} \right|. \quad (76)$$

On the other hand, the measured value of $|\epsilon|$ requires $|\text{Arg}[\Delta m_K]| \approx 6 \times 10^{-3}$. This hierarchy of phases poses a challenge for model-building efforts since it suggests that flavor physics responsible for large dipole operator coefficients can not be the source of CP violation in the Kaon system, especially ϵ .

We have not discussed dipole operator phenomenology in the up quark sector. One issue which might be of concern is the absence of significant $\Delta I = \frac{1}{2}$ enhancement in $D \rightarrow \pi\pi$ decays [80]. However, it should be noted that chromomagnetic dipole operator coefficients in the up sector are, in general, independent of the corresponding down sector coefficients, and could certainly be smaller in magnitude. A naive

estimate indicates that a factor of ~ 3 suppression relative to the down quark coefficients would be sufficient for transitions between the first two families. This assumes that the down quark coefficients account for 30 – 50% of the $\Delta I = \frac{1}{2}$ amplitude in K decays.³²

We have expressed the $\Delta I = \frac{1}{2}$ amplitudes in terms of an unknown $\mathcal{O}(p^2)$ chiral perturbation theory suppression factor, m_K^2/Λ^2 . However, substantial $\Delta I = \frac{1}{2}$ enhancement can be obtained by setting it as low as .2, which is a reasonably conservative estimate. Nevertheless, theoretical progress is essential in calculating chromomagnetic dipole matrix elements. This is certainly also true of the $\Delta S = 2$ matrix elements, some of which play an important role in constraining the dipole-induced $\Delta I = \frac{1}{2}$ amplitude in supersymmetric models. Their ‘bag factors’ have been crudely set to 1, according to the vacuum insertion approximation. We have also not taken into account leading or next-to-leading order QCD corrections of the $\Delta S = 2$ operator coefficients.

Moving to the B system, in the standard model the expected inclusive branching ratio for non-leptonic charmless b decays is $\approx 1 - 2\%$. On the other hand, suppression of $\text{BR}_\ell(B)$ via chromomagnetic dipole operators implies a branching ratio for $b \rightarrow xg$ which is about an order of magnitude larger. Non-leptonic charmless b decays have been observed at CLEO with a branching ratio[6],

$$\text{BR}(B^0 \rightarrow K^+\pi^- + \pi^+\pi^-) = 1.8_{-0.5}^{+0.6} \pm 0.2, \quad (77)$$

which is in good agreement with standard model predictions. It is important to check that in models of $\text{BR}_\ell(B)$ suppression the exclusive rates associated with $b \rightarrow xg$ are not in conflict with this measurement. Of course, such calculations are likely to involve considerable theoretical uncertainty. Ultimately, this issue should be settled by experiment. Perhaps LEP or SLC, with their vertex detector capabilities, could resolve the presence of charm decay vertices in non-leptonic b decays with sufficient efficiency to determine whether charm is not produced 15% – 30% of the time.

We end with a summary of our results. In Section 3 we carried out a model-independent analysis of dipole operator phenomenology which endeavors to study possible connections between $\Delta I = \frac{1}{2}$ enhancement, $\text{BR}_\ell(B)$ suppression, and the quark spectrum. The dipole operator coefficients were therefore parametrized in

³²It is interesting to note that attempts to solve the strong CP problem with a massless up quark would lead to vanishing transition dipole moments between the u and c quarks because of chiral symmetry.

terms of known quark masses and mixing angles. Our results can be classified according to the scale of flavor physics which induces the dipole operators and quark masses. Remarkably, there are essentially two distinct cases in which chromomagnetic dipole operators can lead to direct associations between $\Delta I = \frac{1}{2}$ enhancement, or $\text{BR}_\ell(B)$ suppression, and observed quark masses and mixing angles. For flavor physics in *Region I*, $M \sim 1 - 2 \text{ TeV}$, suppression of $\text{BR}_\ell(B)$ to 10 – 11% is likely to be associated with generation of V_{cb} or m_b . In *Region II*, $M \sim \frac{1}{2} \text{ TeV}$, the analysis suggests that approximately 30 – 50% of the observed $\Delta I = \frac{1}{2}$ amplitude can be directly associated with generation of θ_c or m_s . $\text{BR}_\ell(B)$ suppression can be directly associated with generation of V_{ub} , or with generation of m_b in conjunction with V_{cb} . $\text{BR}_\ell(B)$ suppression will also lead to a decrease in the charm-multiplicity relative to the standard-model prediction, which is consistent with recent measurements.

In Section 4 we showed that supersymmetric models can provide explicit realizations of Region I or II phenomenology. In particular, for weak scale gluinos and squark masses in the 1 – 2 *TeV* range it is possible to tie in $\text{BR}_\ell(B)$ suppression with radiative generation of V_{cb} . For weak scale gluinos and $\sim \frac{1}{2} \text{ TeV}$ squarks it should be possible to obtain $\text{BR}_\ell(B)$ suppression in association with generation of V_{ub} , and 30% – 50% of the $\Delta I = \frac{1}{2}$ amplitude in association with generation of m_s or θ_c . Some tuning between supersymmetric contributions to Δm_K , up to 1 part in 3-4 for the larger $\Delta I = \frac{1}{2}$ enhancements, may be required. For larger squark masses the Δm_K constraints are weaker, but a small tuning of θ_c or m_s would be required. The most appealing scenario arises in Region II, where all left-right down squark mass insertions can be of same order, leading to radiative generation of θ_c , V_{ub} , and m_d , together with $\Delta I = \frac{1}{2}$ enhancement and $\text{BR}_\ell(B)$ suppression. Finally, we saw that $\text{BR}_\ell(B)$ suppression, and even larger $\Delta I = \frac{1}{2}$ amplitudes are possible for ultra-light gluinos, although a connection to the quark mass spectrum is unlikely. Unfortunately, in supergravity theories with general Kahler potential, or in string theory with moduli-driven supersymmetry breaking, off-diagonal left-right squark mass insertions are not large enough to obtain $\text{BR}_\ell(B)$ suppression in Region I, and may not be large enough for $\Delta I = \frac{1}{2}$ enhancement.

In Section 5 we discussed an entirely different class of models in which electroweak symmetry breaking is due to technicolor interactions, and quark masses are due to techniscalar exchange [64]. We found that $\text{BR}_\ell(B)$ suppression is possible for techniscalar masses in Regions I and II, and that 30% – 50% of the $\Delta I = \frac{1}{2}$ amplitude may be generated in Region II. This enhancement is bounded from above by the

magnitudes of m_s , or θ_c . Interestingly, Δm_K constraints are weak and do not play a role. There are many possible connections between $\Delta I = \frac{1}{2}$ enhancement, or $\text{BR}_\ell(B)$ suppression, and the quark spectrum, depending on how many techniscalars or technifermions are introduced. This was summarized in the previous section. We only note that, unlike in radiative models, generation of heavy quark masses also has rich implications for chromomagnetic dipole operator phenomenology. In particular, generation of m_b can be associated with $\text{BR}_\ell(B)$ suppression at either flavor scale. Furthermore, in Region II the top quark acquires a large chromomagnetic dipole moment, which would substantially enhance the Tevatron $t\bar{t}$ production cross section [70]. Finally, we investigated the effects of dimension-6 operators on the $Z \rightarrow b\bar{b}$ decay width and FCNC. We found that R_b receives substantial positive contributions, which are correlated with contributions to $b \rightarrow s\mu^+\mu^-$. For example, for $\frac{\delta R_b}{R_b} \approx 3\%$, one obtains $\text{BR}(b \rightarrow s\mu^+\mu^-) \sim 10^{-5}$.

Techniscalar models are appealing because the dipole moments are automatically tied to the quark mass spectrum. Their magnitudes are determined by the techniscalar mass(es). An important issue for Region II phenomenology is whether techniscalar masses as light as $\frac{1}{2} \text{TeV}$ are consistent with technicolor dynamics. We argued that this is not unreasonable, based on naive estimates of the technifermion constituent mass.

Other models, which we did not discuss, were also investigated. We found that $\Delta I = \frac{1}{2}$ amplitudes due to dipole penguin graphs with charged-Higgs, scalar diquarks, vectorlike quarks, or leptoquarks in the loop tend to be smaller, because of more restrictive Δm_K constraints. In fact, it is difficult to find models which can match the dipole-induced $\Delta I = \frac{1}{2}$ enhancement possible in supersymmetric and techniscalar models. Models of quark substructure are potential candidates [81], since they are likely to produce transition dipole moments in association with quark mass generation, but a fairly light compositeness scale would be required.

We end with implications of $\text{BR}_\ell(B)$ suppression for radiative B decays. A general model-independent criterion, applied at the scale of new flavor physics, distinguishes those models of $\text{BR}_\ell(B)$ suppression which do not conflict with the inclusive measurement of $\text{BR}(b \rightarrow x\gamma)$. We have seen that it can be applied to a rather general class of models with new scalar bosons at the TeV scale. The analysis also suggests that those models which survive in Region II may produce *large rates for* $b \rightarrow d\gamma$. The corresponding branching ratio would lie in the range $10^{-5} - 10^{-4}$, which is substantially larger than the standard model prediction. This is, in fact, the case in both the su-

persymmetric and techniscalar models we have studied. Implications for $B \rightarrow \rho\gamma$, or $B \rightarrow \omega\gamma$ offer another example of the richness of Region II phenomenology. Finally, our main result can be summarized by comparing the model-independent, supersymmetric, and techniscalar plots of Figs. 4, 8, and 12, respectively. Their obvious similarity strongly suggests that substantial $\Delta I = \frac{1}{2}$ enhancement, $\text{BR}_\ell(B)$ suppression, and the quark mass spectrum are tied together by chromomagnetic dipole operators which are induced by new flavor physics at the TeV scale.

ACKNOWLEDGEMENTS

It is a pleasure to thank Michael Peskin for useful and crucial discussions, and for helpful comments regarding the manuscript. I would also like to thank John Donoghue for a discussion of $\Delta I = \frac{1}{2}$ dipole operator matrix elements, and Michael Dine, Adam Falk, Matthias Neubert, Yossi Nir and Michal Porat for useful conversations. Thanks are also due to Joanne Hewett, Tom Rizzo, Sheldon Stone and Steve Wagoner for help with experimental issues.

Appendix A. More on Connections to the Quark Mass Spectrum

Throughout this paper we have expressed the physical transition dipole operators in terms of partial contributions to the down quark mass matrix, in the mass eigenstate basis. In order to study the connection between these contributions and known features of the quark spectrum it is necessary to reexpress them in terms of mass contributions in the quark interaction basis. This task is simplified if we make some reasonably general assumptions about the form of the full down quark mass matrix, M^d , after all individual contributions have been taken into account. In particular, we always assume that an interaction basis exists in which the entries $M_{ij}^d \bar{d}_L^i d_R^j$ satisfy the hierarchy

$$M^d = \begin{pmatrix} \sim m_d & \sim m_d & \sim m_d \\ \sim m_d & \sim m_s & \sim m_s \\ \sim m_d & \sim m_s & \sim m_b \end{pmatrix}, \quad (A1)$$

with similar assumptions for the up quark matrix. Eq. (A1) is intended to be schematic. For example, the (12) entry will actually be $\approx \theta_c m_s$ which is several times larger than m_d . Given eq. (A1) and its analogue for the up sector, the KM angles will essentially be generated in the down sector.³³

Diagonalization of eq. (A1) is straightforward. The down quark masses are given by

$$m_d \approx m_{11} - \frac{m_{12}m_{21}}{m_s}, \quad m_s \approx m_{22} - \frac{m_{23}m_{32}}{m_b}, \quad m_b \approx m_{33}. \quad (A2)$$

The down quark mass eigenstates are given in terms of the interaction basis by

$$|\psi_L^i\rangle = x_{ij}^L |d_L^j\rangle, \quad |\psi_R^i\rangle = x_{ij}^R |d_R^j\rangle, \quad (A3)$$

where $\psi_L^1, \psi_L^2, \psi_L^3$ are the left-handed quark mass eigenstates d_L, s_L, b_L , respectively, and R subscripts label the corresponding right-handed quarks. Taking all parameters to be real, the x_L^{ij} are given by

$$x_{ii}^L \approx 1, \quad x_{21}^L \approx \frac{m_{12}}{m_{22}} \approx V_{us}, \quad x_{32}^L \approx \frac{m_{23}}{m_{33}} \approx V_{cb}, \quad x_{31}^L \approx \frac{m_{13}}{m_{33}} \approx V_{ub},$$

$$x_{12}^L \approx -x_{21}^L, \quad x_{23}^L \approx -x_{32}^L, \quad x_{13}^L \approx -\frac{m_{13}}{m_b} + \frac{m_{23}}{m_{33}} \frac{m_{12}}{m_{22}} \approx V_{td}. \quad (A4)$$

³³The (32) and (31) entries in eq. (A1) are unrelated to the KM angles and, in general, can be as large as a few GeV. However, in this case the connection between quark masses, or mixing angles, and $\text{BR}_\ell(B)$ suppression is lost.

Expressions for the x_{ij}^R are obtained from the above by interchanging indices on the m_{ij} . The up quark masses and eigenstates are completely analogous. Note that

$$V_{ts} \approx -V_{cb}, \quad V_{td} \approx -V_{ub} + V_{cb}V_{us} \quad (A5)$$

in the limit of a diagonal up matrix.

We can now investigate claims made in Section 3 about the correspondence between certain ranges for the off-diagonal down quark mass matrix contributions, in the mass eigenstate basis, and generation of observed features of the quark spectrum. Recall that the parametrization of Section 3, eq. (24), corresponds to generation of rank-1 dipole operator coefficient matrices, C_G^{ij} , and proportional rank-1 mass matrices Δm_{ij} . In general, there may be several such contributions, each one generated by a different exchange of particles. We assume that these do not upset the hierarchy in (A1), so that large cancelations among different contributions to the mass matrix are not required.

(a) $|\Delta m_{ds}^+| \sim |\theta_c m_s|$ can be associated with generation of θ_c , or m_s , but not both. This can be seen by expressing Δm_{ds}^+ in the interaction basis,

$$\Delta m_{ds}^+ = \Delta m_{12} - \frac{m_{12}}{m_{22}} \Delta m_{22} + \mathcal{O}(\theta_c m_d). \quad (A6)$$

If Δm_{12} accounts for the bulk of m_{12} then the induced mass matrix generates θ_c . Alternatively, if Δm_{22} accounts for the bulk of m_{22} , then it generates m_s . In either case one obtains $|\Delta m_{ds}^+| \sim |\theta_c m_s|$. However, the limit in which both θ_c and m_s are generated by Δm_{ij} leads to suppression of $|\Delta m_{ds}^+|$.

(b) $|\Delta m_{sb}^+| \sim |V_{cb} m_b|$ can be associated with generation of V_{cb} , or m_b , but not both. In the interaction basis

$$\Delta m_{sb}^+ = \Delta m_{23} - \frac{m_{23}}{m_{33}} \Delta m_{33} + \mathcal{O}(V_{cb} m_s). \quad (A7)$$

If Δm_{23} accounts for the bulk of m_{23} then the induced mass matrix generates V_{cb} . Alternatively, if Δm_{33} accounts for the bulk of m_{33} , then the induced mass matrix generates m_b . In either case one obtains $|\Delta m_{sb}^+| \sim |V_{cb} m_b|$. However, if both V_{cb} and m_b are generated by Δm_{ij} , then $|\Delta m_{sb}^+|$ is suppressed. For example, if

$$m_{33} - \Delta m_{33} \sim V_{cb} m_b, \quad m_{23} - \Delta m_{23} \sim V_{ub} m_b, \quad (A8)$$

then $|\Delta m_{sb}^+| \sim |V_{ub}m_b|$.

(c) $|\Delta m_{db}^+| \sim |V_{ub}m_b|$ can be associated with generation of V_{ub} , V_{cb} , or m_b , but not all three. In the interaction basis

$$\Delta m_{db}^+ = \Delta m_{13} - \frac{m_{12}}{m_{22}}\Delta m_{23} - \frac{m_{13}}{m_{33}}\Delta m_{33} + \mathcal{O}(V_{cb}V_{ub}m_b) \quad (\text{A9})$$

If Δm_{ij} generates V_{ub} , V_{cb} , or m_b then it must account for the bulk of m_{13} , m_{23} , or m_{33} , respectively. Clearly, if any one, or any two of these possibilities is true, one obtains $|\Delta m_{db}^+| \sim |V_{ub}m_b|$. However, in the limit that all three are true, $|\Delta m_{db}^+|$ is much smaller.

It is clear from (b) and (c) that $\xi' \sim .1$ (see eq. (34)) can correspond to generation of V_{cb} in conjunction with m_b , or to generation of V_{ub} , whereas $\xi' \sim 1$ (see eq. (33)) can correspond to generation of V_{cb} or m_b , but not both.

Supersymmetry

We saw that in supersymmetric models Δm_{ij} is generally rank-3, but still proportional to the dipole moment matrices, up to very small corrections. The only change to the above analysis is that radiative generation of m_b is not an option. This means, in particular, that Region II scenarios of $\text{BR}_\ell(B)$ suppression can be associated with generation of V_{ub} , but not V_{cb} .

An issue of relevance for $\Delta I = \frac{1}{2}$ enhancement with *ultra-light gluinos* is how large a hierarchy between $\delta\tilde{m}_{d_L s_R}^2$ and $\delta\tilde{m}_{d_R s_L}^2$ is possible, for the purposes of evading Δm_K constraints. According to Figs. 6 and 9, large enhancement requires a hierarchy of $\mathcal{O}(30)$ for weak scale squarks, and $\mathcal{O}(300)$ for squarks near a TeV. To settle this issue it is useful to express the squark mass insertions in the quark interaction basis,

$$\begin{aligned} \delta\tilde{m}_{d_L s_R}^2 &\approx \delta\tilde{m}_{1_L 2_R}^2 + x_{12}^L \delta\tilde{m}_{2_L 2_R}^2 + x_{21}^R \delta\tilde{m}_{1_L 1_R}^2 + x_{12}^L x_{21}^R \delta\tilde{m}_{2_L 1_R}^2 + \dots \\ \delta\tilde{m}_{d_R s_L}^2 &\approx \delta\tilde{m}_{2_L 1_R}^2 + x_{12}^R \delta\tilde{m}_{2_L 2_R}^2 + x_{21}^L \delta\tilde{m}_{1_L 1_R}^2 + x_{12}^R x_{21}^L \delta\tilde{m}_{1_L 2_R}^2 + \dots \end{aligned} \quad (\text{A10})$$

Terms involving 3rd generation squark mass insertions have not been shown explicitly. Given eq. (A1), a hierarchy of $\mathcal{O}(30)$ requires a similar hierarchy between $\delta\tilde{m}_{1_L 2_R}^2$ and $\delta\tilde{m}_{2_L 1_R}^2$, and an order of magnitude hierarchy between $\delta\tilde{m}_{1_L 2_R}^2$, and both $\delta\tilde{m}_{2_L 2_R}^2$ and $\delta\tilde{m}_{1_L 1_R}^2$. So in scenarios with ultra-light gluinos and weak scale squarks several non-trivial conditions must be satisfied. Assuming that the bulk of θ_c is generated in the down sector, an upper bound on the ratio of $\delta\tilde{m}_{d_L s_R}^2$ to $\delta\tilde{m}_{d_R s_L}^2$ of $\mathcal{O}(400)$,

corresponding to $(x_{12}^R x_{21}^L)^{-1}$, is obtained by setting all squark mass insertions to zero except $\delta\tilde{m}_{1_L 2_R}^2$. We have used a lower bound for x_{12}^R of $\mathcal{O}(\frac{m_d}{m_s}\theta_c)$, obtained in the limit that the m_{21} entry of the down quark mass matrix vanishes. Strictly speaking, scenarios with ultra-light gluinos and squarks near a TeV are possible, but they are highly constrained and clearly disfavored, even though they may lead to generation of θ_c , as noted in Section 4.

Techniscalar models

In techniscalar models in which both third and second generation masses are due to techniscalar exchange the down quark mass matrix is generally of the form

$$M^d = m_3|h_L^3\rangle\langle h_R^3| + m_2|h_L^2\rangle\langle h_R^2| + \delta M. \quad (A11)$$

The bras and kets are dimensionless 3-component vectors, normalized to unity, obtained from Yukawa coupling vectors like \mathbf{h} , \mathbf{h}^d in (66). The massive coefficients have magnitudes $m_3 \sim m_b$, $m_2 \sim m_s$, and the matrix δM is generally rank 3 or less, with entries which are typically $\mathcal{O}(m_d)$, or $\mathcal{O}(\theta_c m_s)$. For example, if 1st generation masses and mixing angles are also due to techniscalar exchange then δM is rank 1, however, if they are due to some radiative mechanism then δM might be rank 3. The up quark matrix is of the same form. $SU(2)_L$ implies that $|h_L^3\rangle$ and $|h_L^2\rangle$ are equal for the up and down matrices,³⁴ which insures the near alignment of up and down mass eigenstates required by the KM mixing hierarchy.

It is easy to show that the following interaction basis reproduces the hierarchy in (A1) for M^d :

$$|3_L\rangle = |h_L^3\rangle, \quad |2_L\rangle \propto |h_L^2\rangle - |h_L^3\rangle\langle h_L^3|h_L^2\rangle, \quad |1_L\rangle \perp |2_L\rangle, |3_L\rangle. \quad (A12)$$

The right-handed basis elements are completely analogous. Note, in particular, that the first two terms in (A11) correspond to the lower right 2×2 submatrix of eq. (A1) up to corrections due to δM . This explains item (b) at the end of Section 5, since with two sets of technifermions ($N_D = 2$) and a single techniscalar the dipole operator coefficient matrices are proportional to the sum of the first two terms. This means that transition dipole moments must be proportional to matrix elements of δM , leading to Region II phenomenology. If only 3rd generation masses are due to

³⁴For two copies of the technifermions T_R , U_L , D_L and a single techniscalar, this also assumes that the up and down condensates respect custodial isospin symmetry which, of course, is also required by the ρ parameter constraint.

techniscalar exchange then M^d can still be written in the form of (A10), but only the first term would be due to techniscalar exchange, accounting for the bulk of the (33) entry in eq.(A1). This explains item (a), since the dipole coefficients would be proportional to the first term in eq. (A10), leading to Region I phenomenology. Similarly, in the case of item (c) the dipole coefficient matrices correspond to a sum of two distinct contributions, proportional to the first and second terms in (A10), respectively. In the absence of substantial accidental cancelations, each of these contributions leads to Region I phenomenology. Finally, in (d) the dipole coefficients are proportional to δM , again leading to Region II phenomenology.

Appendix B. New contributions to Δm_K and Δm_B

Supersymmetry

The supersymmetric contributions to Δm_K are given by³⁵ [54]

$$\begin{aligned} \Delta m_K = & \frac{\alpha_s^2}{216m_{\tilde{q}}^2} \left(\frac{2}{3} f_K^2 m_K \right) \left[\left(\frac{\delta\tilde{m}_{d_L s_R}^4}{m_{\tilde{q}}^4} \right) 216 R_K x f_6(x) \right. \\ & + \left(\frac{\delta\tilde{m}_{d_R s_L}^4}{m_{\tilde{q}}^4} \right) 216 R_K x f_6(x) + \left(\frac{\delta\tilde{m}_{d_L s_R}^2}{m_{\tilde{q}}^2} \frac{\delta\tilde{m}_{d_R s_L}^2}{m_{\tilde{q}}^2} \right) 108 \tilde{f}_6(x) \\ & - \left(\frac{\delta\tilde{m}_{d_L s_L}^4}{m_{\tilde{q}}^4} + \frac{\delta\tilde{m}_{d_R s_R}^4}{m_{\tilde{q}}^4} \right) (66 \tilde{f}_6(x) + 24 x f_6(x)) \\ & \left. + \left(\frac{\delta\tilde{m}_{d_L s_L}^2}{m_{\tilde{q}}^2} \frac{\delta\tilde{m}_{d_R s_R}^2}{m_{\tilde{q}}^2} \right) ([-36 + 24 R_K] \tilde{f}_6(x) - [72 + 384 R_K] x f_6(x)) \right], \quad (B1) \end{aligned}$$

where $f_K = 161 \text{ MeV}$, $x = m_g^2/m_{\tilde{q}}^2$,

$$R_K \equiv \left(\frac{m_K}{m_s + m_d} \right)^2,$$

and

$$\begin{aligned} f_6(x) &= \frac{1}{6(1-x)^5} (-6 \ln x - 18 x \ln x - x^3 + 9x^2 + 9x - 17) \\ \tilde{f}_6(x) &= \frac{1}{3(1-x)^5} (-6x^2 \ln x - 6x \ln x + x^3 + 9x^2 - 9x - 1). \end{aligned}$$

³⁵ The signs of all terms which include the enhancement factor R_K are opposite to those in [54]. The source of the discrepancy is in the vacuum insertion matrix elements which have been used. Our matrix elements are consistent with ref. [82].

We have used the vacuum insertion approximation for all matrix elements, with $m_s = 150 \text{ MeV}$ and $m_d = 8 \text{ MeV}$. α_s , $m_{\tilde{g}}$ and $m_{\tilde{q}}$ are taken at the squark mass scale, and QCD corrections are not included. Supersymmetric contributions to Δm_B in the vacuum insertion approximation are obtained from (B1) via the appropriate flavor substitutions. We have taken $f_B \approx 230 \text{ MeV}$, and $m_b = 4.25 \text{ GeV}$ in R_B , corresponding to the running mass $m_b(m_b)$.

Techniscalar models

We give a crude estimate for the contributions to Δm_K of box graphs with techniscalars and technifermions in the loop in the vacuum insertion approximation, without QCD corrections. The technifermions are assigned a mass m_{TC} , equal to the ‘constituent’ mass in eq. (69). The simplest case is considered, corresponding to $N_D = 1$, and exchange of a single techniscalar ω . The $N_D = 2$ case is slightly more restrictive, but our conclusions do not change significantly. We obtain

$$\begin{aligned} \Delta m_K = & \frac{N_{TC} m_K f_K^2}{12} \left[\left(\frac{\lambda_d^2 \bar{\lambda}_s^2}{2} + \frac{\bar{\lambda}_d^2 \lambda_s^2}{2} \right) \frac{z^2}{m_{TC}^2} I(z) R_K + (\lambda_d^2 \lambda_s^2 + \bar{\lambda}_d^2 \bar{\lambda}_s^2) \frac{\tilde{I}(z)}{m_\omega^2} \right. \\ & \left. + \lambda_d \lambda_s \bar{\lambda}_d \bar{\lambda}_s \left(\frac{z}{m_\omega^2} I(z) [2R_K + 3] - \frac{\tilde{I}(z)}{m_\omega^2} \left[\frac{3}{2} R_K + \frac{1}{4} \right] \right) \right], \end{aligned} \quad (B2)$$

where $z = m_{TC}^2/m_\omega^2$, and

$$I(z) = \frac{1}{16\pi^2} \frac{-2 + 2z - (1+z)\ln z}{(1-z)^3}$$

$$\tilde{I}(z) = \frac{1}{16\pi^2} \frac{z^2 - 1 - 2z\ln z}{(1-z)^3}.$$

References

- [1] W.A. Bardeen, A.J. Buras and J.-M. Gerard, *Phys. Lett.* **B 192** (1987) 138.
- [2] A. Pich and E. de Rafael, *Nucl. Phys.* **B 358** (1991) 311.
- [3] A. J. Buras, M. Jamin, and M. E. Lautenbacher, *Nucl. Phys.* **B 408** (1993) 209.
- [4] M. Neubert and B. Stech, *Phys. Lett.* **B 231** (1989) 477; *Phys. Rev.* **D 44** (1991) 775.
- [5] N. Isgur et al., *Phys. Rev. Lett.* **64** (1990) 161.
- [6] V. Sharma, talk given at DPF '94, Albuquerque, New Mexico, August, 1994.
- [7] G. Altarelli and S. Petrarca, *Phys. Lett.* **B 261B** (1991) 303.
- [8] G. Altarelli and L. Maiani, *Phys. Lett.* **B 52B** (1974) 351.
- [9] M. K. Gaillard and B. Lee, *Phys. Rev. Lett.* **33** (1974) 108.
- [10] G. Altarelli et al., *Phys. Lett.* **B 99** (1981) 141; *Nucl. Phys.* **B 187** (1981) 461.
- [11] A. J. Buras, P. H. Weisz, *Nucl. Phys.* **B 333** (1990) 66.
- [12] I. Bigi et al., CERN preprint CERN- TH.7082/93.
- [13] A.F. Falk, M.B. Wise and I. Dunietz, Fermilab preprint, FERMILAB-PUB-94-106-T.
- [14] F. Muheim, talk given at DPF '94, Albuquerque, New Mexico, August, 1994.
- [15] H. Fritzsch and P. Minkowski, *Phys. Lett.* **B 61B** (1976) 275.
- [16] R. K. Ellis, *Nucl. Phys.* **B 106** (1976) 239.
- [17] A. I. Vainshtein, V. I. Zakharov, and M. A. Shifman, *JETP* (Sov. Phys.) **45** (1977) 670.
- [18] C. T. Hill, *Nucl. Phys.* **B 156** (1979) 417.
- [19] E. Ma, *Phys. Rev. Lett.* **57** (1986) 287.
- [20] E. Papantonopoulos, N. D. Tracas and G. Zoupanos, *Phys. Lett.* **B 188** (1987) 493.
- [21] J. F. Donoghue and B. R. Holstein, *Phys. Rev.* **D 32** (1985) 1152.
- [22] B. G. Grzadkowski and W.-S. Hou, *Phys. Lett.* **B 272** (1991) 383.
- [23] B. Barish et al., CLEO Collaboration, CLEO report CLEO CONF 94-1, 1994.

- [24] C.Q. Geng, P. Turcotte and W.S. Hou, National Taiwan University preprint, NHCU-HEP-94-17A.
- [25] J. L. Hewett, *Phys. Rev. Lett.* **70** (1993) 1045.
- [26] V. Barger, M.S. Berger, and R.J.N. Phillips, *Phys. Rev. Lett.* **70** (1993) 1368.
- [27] K. Hikasa et al., Particle Data Book, *Phys. Rev. D* **45** (1992) I1.
- [28] M. Jamin and A. Pich, CERN preprint, CERN-TH.7151/94.
- [29] J. L. Cortes, X. Y. Pham and A. Tounsi, *Phys. Rev. D* **D25** (1982) 188.
- [30] R. E. Behrends, R. J. Finkelstein and A. Sirlin, *Phys. Rev.* **101** (1956) 866.
- [31] N. Cabibbo and L. Maiani, *Phys. Lett.* **B 79** (1978) 109.
- [32] R. Ruckl, in: *Heavy Flavors at LEP*, CERN Yellow Report 89-08, Vol. 1 (CERN, Geneva, 1989).
- [33] Z. Ligeti and Y. Nir, *Phys. Rev. D* **49** (1994) 4331.
- [34] C. T. H. Davies et. al., Ohio State University preprint, OHSTPY-HEP-T-94-004.
- [35] W. F. Palmer and B. Stech, *Phys. Rev. D* **48** (1993) 4174.
- [36] A. I. Vainshtein, V. I. Zakharov, and M. A. Shifman, *JETP Lett.* **23** (1976) 602.
- [37] See, for example, G. Cella, et al., *Phys. Lett.* **B 248** (1990) 181; R. Grigjanis, et al., *Phys. Lett.* **B 213** (1988) 355; *Phys. Lett.* **B 237** (1990) 252; M. Misiak, *Phys. Lett.* **B 269** (1991) 161; *Nucl. Phys.* **B 393** (1993) 23; B. Grinstein, et al., *Phys. Lett.* **B 202** (1988) 138; *Nucl. Phys.* **B 339** (1990) 269; M. Ciuchini, et al., *Phys. Lett.* **B 316** (1993) 127.
- [38] H.-Y. Cheng, *Phys. Rev. D* **34** (1986) 1397.
- [39] A. Manohar and H. Georgi, *Nucl. Phys.* **B 234** (1984) 189.
- [40] J. F. Donoghue, E. Golowich, and B. R. Holstein, *Phys. Rev. D* **30** (1984) 587.
- [41] J. Bijnens, *Phys. Lett.* **B 152** (1985) 226.
- [42] J. Kambor, J. Missimer, and D. Wyler, *Phys. Lett.* **B 261** (1991) 496.
- [43] S. Bertolini, M. Fabbrichesi, and E. Gabrielli, CERN preprint CERN- TH.7097/93.
- [44] M. Kremer and G. Schierholz, *Phys. Lett.* **B 283** (1987) 283.
- [45] S. Narison, *Phys. Lett.* **B 210** (1988) 238.
- [46] E. Golowich and B.R. Holstein, *Phys. Rev. Lett.* **35** (1975) 831.

- [47] H.P. Nilles, *Phys. Rep.* **110** (1984) 1.
- [48] M. Dine, A. Kagan and R. Leigh, *Phys. Rev. D* **48** (1993) 4269.
- [49] Y. Nir and N. Seiberg, *Phys. Lett. B* **309** (1993) 337.
- [50] J.-M. Gerard, W. Grimus, and A. Raychaudhuri, *Phys. Lett. B* **145** (1984) 400.
- [51] S. Bertolini et al., *Nucl. Phys. B* **353** (1991) 591.
- [52] M. Dugan, B. Grinstein and L. Hall, *Nucl. Phys. B* **255** (1985) 413.
- [53] F. Gabbiani and A. Masiero, *Nucl. Phys. B* **322** (1989) 235.
- [54] J. S. Hagelin, S. Kelley, and T. Tanaka, *Nucl. Phys. B* **415** (1994) 293.
- [55] H. E. Haber, *SUSY-93 Workshop*, Northeastern University, April 1993 and UCSC preprint SCIPP 93/21.
- [56] C. Albajar et al., UA1 Collaboration, *Phys. Lett. B* **198** (1987) 261.
- [57] L. Clavelli, *Phys. Rev. D* **46** (1992) 2112; L. Clavelli, P. Coulter, and K. Yuan, *Phys. Rev. D* **47** (1993) 1973.
- [58] M. Jezabek and J. H. Kuhn, *Phys. Lett. B* **301** (1993) 121.
- [59] G. B. Bhattacharyya and A. Raychaudhuri, *Phys. Rev. D* **49** (1994) R1156; F. De Campos and J. W. F. Valle, Universitat de Valencia preprint, FTUV/93- 9a; M. Schmelling and R. D. St.Denis, *Phys. Lett. B* **329** (1994) 393; M. B. Cakir and G. R. Farrar, Rutgers University preprint RU-94- 04; M. Diaz, Vanderbilt University preprint, VAND-TH-94-7.
- [60] V. Kaplunovsky and J. Louis, *Phys. Lett. B* **306** (1993) 269.
- [61] R. Barbieri, J. Louis and M. Moretti, *Phys. Lett. B* **312** (1993) 451.
- [62] A. Kagan, in *Proceedings of Recent Advances in the Superworld*, HARC, Texas, April 1993.
- [63] S.K. Soni and H.A. Weldon, *Phys. Lett. B* **126** (1983) 215.
- [64] A.L. Kagan, in *Proceedings of the 15th Johns Hopkins Workshop on Current Problems in Particle Physics*, Baltimore, Maryland 1991.
- [65] S. Dimopoulos and L. Susskind, *Nucl. Phys. B* **155** (1979) 237; E. Eichten and K. Lane, *Phys. Lett. B* **90** (1980) 125.
- [66] M. Dine, A.L. Kagan and S. Samuel, *Phys. Lett. B* **243** (1990) 250.

- [67] G.'t Hooft, Lecture at Cargese Summer Institute, 1979, in *Recent Developments in Gauge Theories*, edited by G.'t Hooft et al. (Plenum Press, New York, 1980); E.H. Simmons, *Nucl. Phys.* **B 312** (1989) 253; S. Samuel, *Nucl. Phys.* **B 341** (1990) 513.
- [68] R.S. Chivukula, *Phys. Rev. Lett.* **61** (1988) 2657.
- [69] L. Randall and R. Sundrum, *Phys. Lett.* **B 312** (1993) 148.
- [70] D. Atwood, A. Kagan and T.G. Rizzo, SLAC preprint SLAC-PUB-6580, July 1994, T/E.
- [71] F. Abe, et al., CDF Collaboration, Fermilab report Fermilab-PUB-94/097-E, 1994.
- [72] R.S. Chivukula, S.B. Selipsky and E.H. Simmons, *Phys. Rev. Lett.* **69** (1992) 575.
- [73] R.S. Chivukula et al., *Phys. Lett.* **B 311** (1993) 157.
- [74] B. Grinstein, Y. Nir and J.M. Soares, *Phys. Rev.* **D 48** (1993) 3960.
- [75] R.S. Chivukula, E.H. Simmons, and J. Terning, Boston University preprint, BUHEP-94-8.
- [76] H. Georgi, *Weak Interactions and Modern Particle Theory* (Benjamin-Cummings, Menlo Park, 1984), p. 77.
- [77] D. Schaile, talk given at the 27th International Conference on High Energy Physics, Glasgow, July, 1994.
- [78] C. Albajar et al., UA1 Collaboration, *Phys. Lett.* **B 262** (1991) 163.
- [79] B. Grinstein, M. Savage and M. Wise, *Nucl. Phys.* **B 319** (1989) 271.
- [80] M. Selen et al., CLEO Collaboration, *Phys. Rev. Lett.* **71** (1993) 1973.
- [81] See, e.g., M. Peskin, in *Proceedings of the International Symposium on Lepton and Photon Interactions at High Energies, Bonn, 1981* edited by W. Pfeil (Physikalisches Institut, Universitat Bonn, 1981), p. 880.
- [82] J.Trampetic, *Phys. Rev.* **D 27** (1983) 1565.

Figure Captions

- Figure 1. Parton-model predictions for $\text{BR}_\ell(B)$ versus $\alpha_s(M_z)$, evaluated at $\mu = m_b$.
(a) $m_b = 4.9 \text{ GeV}$, $m_c = 1.4 \text{ GeV}$, (b) $m_b = 4.8 \text{ GeV}$, $m_c = 1.4 \text{ GeV}$, (c) $m_b = 4.7 \text{ GeV}$, $m_c = 1.35 \text{ GeV}$, (d) $m_b = 4.6 \text{ GeV}$, $m_c = 1.2 \text{ GeV}$.
- Figure 2. Contours of $\text{BR}_\ell(B) = .11$ (solid), $.10$ (dashed) in the plane of $|\zeta_G \xi'|$ vs. M for $m_t = 170 \text{ GeV}$, $m_b = 4.8 \text{ GeV}$, $m_c = 1.4 \text{ GeV}$, and $\Lambda^{(4)} = 300 \text{ MeV}$.
- Figure 3. The ratio $\frac{\zeta_F}{\zeta_G}$ vs. M , for different values of $\text{BR}_\ell(B)$, $\text{BR}(b \rightarrow x\gamma)$, and $\text{sign}(\zeta_F) = -\text{sign}(\zeta_G)$ (solid lines), $\text{sign}(\zeta_F) = \text{sign}(\zeta_G)$ (dashed lines). Curves (a),(b),(e),(f) and (c),(d),(g),(h) correspond to $\text{BR}(b \rightarrow x\gamma) = 2 \times 10^{-4}$ and 4×10^{-4} , respectively. $\text{BR}_\ell(B) = .10$ in (a),(c),(e),(g) and $.11$ in (b),(d),(f),(h). $m_b = 4.8 \text{ GeV}$, $m_t = 170 \text{ GeV}$, and $\Lambda^{(4)} = 300 \text{ MeV}$.
- Figure 4. Contours, from top to bottom, of $R_0 = (1.5, 1.0, .7) \frac{m_K^2}{\Lambda^2}$ (solid curves), in the plane of $|\zeta_G(\xi_{ds}^+ - \xi_{ds}^-)|$ vs. M , and contours of $\text{BR}_\ell(B) = .10, .11$ (dashed) in the plane of $|\zeta_G \xi'|$ vs. M plane. We've taken $m_s(m_c) = 150 \text{ MeV}$, $m_c = 1.4 \text{ GeV}$, $m_b = 4.8 \text{ GeV}$, $m_t = 170 \text{ GeV}$ and $\Lambda^{(4)} = 300 \text{ MeV}$.
- Figure 5. Gluino penguin graphs giving rise to chromomagnetic transition dipole moments. The gluon is attached in all possible ways.
- Figure 6. Upper bounds on $\frac{\delta \tilde{m}_{dL}^4}{m_{\tilde{q}}^6}$ (solid) and $\frac{\delta \tilde{m}_{dL}^2 \delta \tilde{m}_{dR}^2}{m_{\tilde{q}}^6}$ (dashed) from gluino box-graph contributions to Δm_K .
- Figure 7. (a) Contours of $\Delta m_K = \Delta m_K^{exp}$ (solid), $2\Delta m_K^{exp}$ (dotted), $3\Delta m_K^{exp}$ (dashed) in the plane of R_0 vs. $m_{\tilde{q}}$. In each case, $m_{\tilde{g}}(m_{\tilde{q}}) = 125, 150, 175, 200, 300 \text{ GeV}$, from top to bottom. $\Lambda^{(4)} = 300 \text{ MeV}$, $m_t = 170 \text{ GeV}$, $m_b = 4.8 \text{ GeV}$, $m_c = 1.4 \text{ GeV}$ and $m_s(m_c) = 150 \text{ MeV}$. (b) Contours of $\Delta m_K = \Delta m_K^{exp}$ (solid), $3\Delta m_K^{exp}$ (dashed) in the plane of $\tilde{m}_{dLsR}(m_{\tilde{q}})$ vs. $m_{\tilde{q}}$. The gluino masses increase from top to bottom. (c) Contours of $\Delta m_K = \Delta m_K^{exp}$ (solid), $3\Delta m_K^{exp}$ (dashed) in the plane of Δm_{ds}^+ vs. $m_{\tilde{q}}$. Gluino masses decrease from top to bottom.
- Figure 8. Contours of $R_0 = (1.5, 1.25, 1.0, .75) \frac{m_K^2}{\Lambda^2}$ (solid) and $\Delta m_K = 3\Delta m_K^{exp}, 2\Delta m_K^{exp}, \Delta m_K^{exp}$ (dashed) in the plane of ξ_{ds}^+ vs. $m_{\tilde{q}}$. R_0 and Δm_K decrease from top to bottom. Also included are contours of $\text{BR}_\ell(B) = .10, .11$ in the plane of ξ' vs. $m_{\tilde{q}}$ (dot-dashed). The quark mass thresholds and $\Lambda^{(4)}$ are as in Fig. 7.

Figure 9. Figs. 9a,b,c are the same as Figs. 7a,b,c, but for $m_{\tilde{g}} = 1, 2, 3, 4 \text{ GeV}$. Gluino masses increase from top to bottom for each value of Δm_K in 9a, 9b, but decrease in 9c. Evolution from $m_{\tilde{q}}$ to m_c is for $\alpha_s(M_z) = .124$, and the usual quark mass thresholds.

Figure 10. (a) Contours of $\text{BR}_\ell(B) = .10, .11$ in the plane of $\Delta m'(m_c)$ vs. $m_{\tilde{q}}$. (b) Contours of $\text{BR}_\ell(B) = .10, .11$ in the plane of $\tilde{m}'(m_{\tilde{q}})$ vs. $m_{\tilde{q}}$, together with upper bounds (thick curves) on $\tilde{m}_{d_L b_R}(m_{\tilde{q}})$ from Δm_B . (c) Contours of $\text{BR}_\ell(B) = .10, .11$ in the plane of $\text{BR}(b \rightarrow x\gamma)$ vs. $m_{\tilde{q}}$. In (a)-(c) the gluino masses are $m_{\tilde{g}}(m_{\tilde{g}}) = 125 \text{ GeV}$ (dashed), 200 GeV (solid), 300 GeV (dot-dashed). Evolution from $m_{\tilde{q}}$ is for $\Lambda^{(4)} = 300 \text{ MeV}$ and the usual quark mass thresholds.

Figure 11. Figs. 11a,b are the same as Figs. 10a,b for $m_{\tilde{g}} = 4 \text{ GeV}$ (solid) and 1 GeV (dashed). Evolution from $m_{\tilde{q}}$ is for $\alpha_s(M_z) = .124$, and the usual quark mass thresholds.

Figure 12. (a) Contours of $R_0 = (1.5, 1.25, 1.0, .75)\frac{m_K^2}{\Lambda^2}$ (solid) in the plane of ξ_{ds}^+ vs. $m_{\tilde{q}}$, and contours of $\text{BR}_\ell(B) = .10, .11$ (dashed) in the plane of $|\xi'|$ vs. $m_{\tilde{q}}$. $\Lambda^{(4)} = 300 \text{ MeV}$, $m_t = 170 \text{ GeV}$, $m_b = 4.8 \text{ GeV}$, $m_c = 1.4 \text{ GeV}$ and $m_s(m_c) = 150 \text{ MeV}$. (b) Contours of $R_0 = (1.5, 1.25, 1.0, .75)\frac{m_K^2}{\Lambda^2}$ (solid) and $\Delta m_K = \Delta m_K^{\text{exp}}$ (dashed) in the plane of $|\lambda_d \bar{\lambda}_s - \bar{\lambda}_d \lambda_s|$ vs. m_ω , for $N_D = 1$ and $N_{TC} = 4$. (c) Contours of $\text{BR}_\ell(B) = .10, .11$ in the plane of $\text{BR}(b \rightarrow x\gamma)$ vs. m_ω .

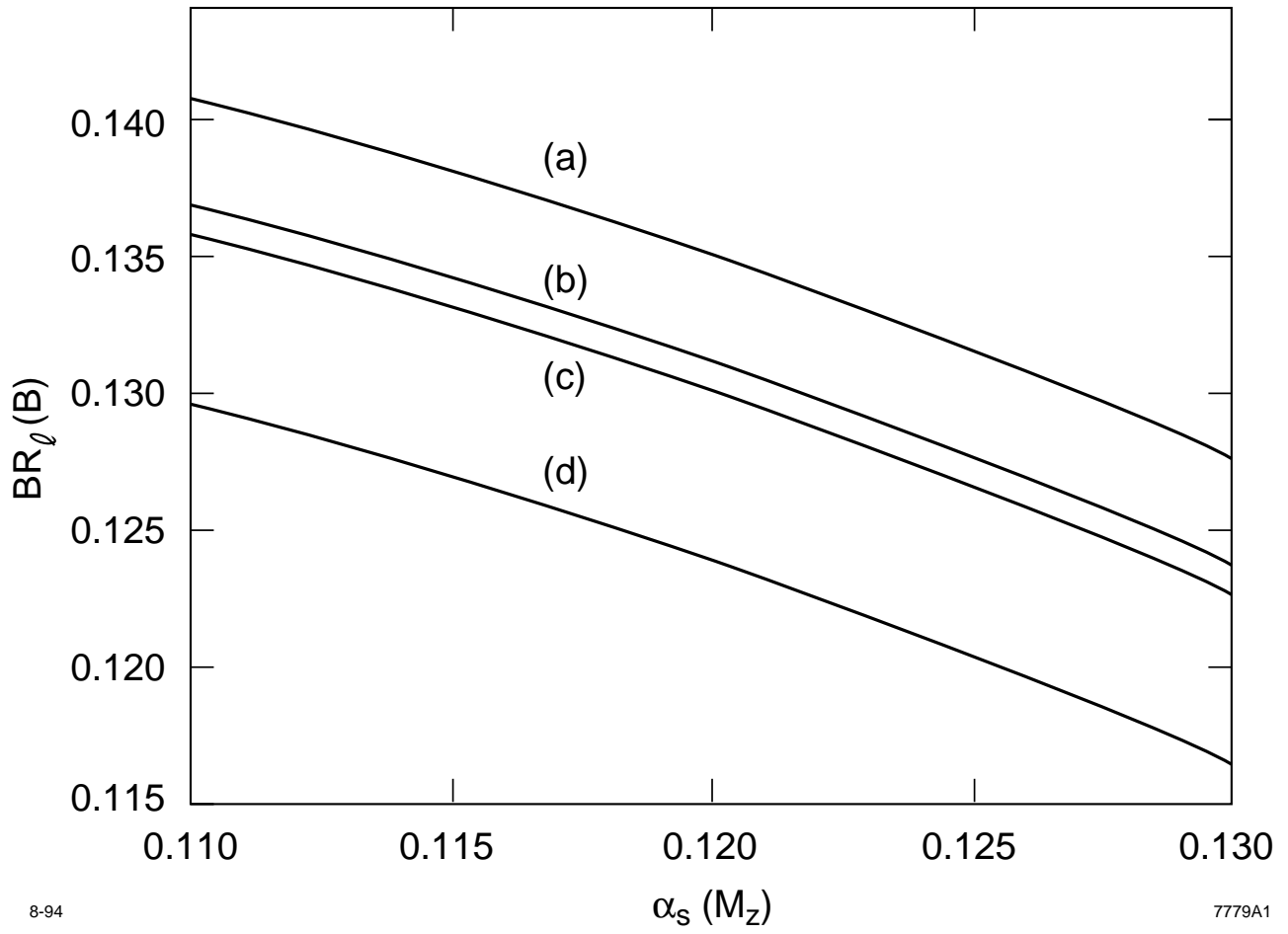
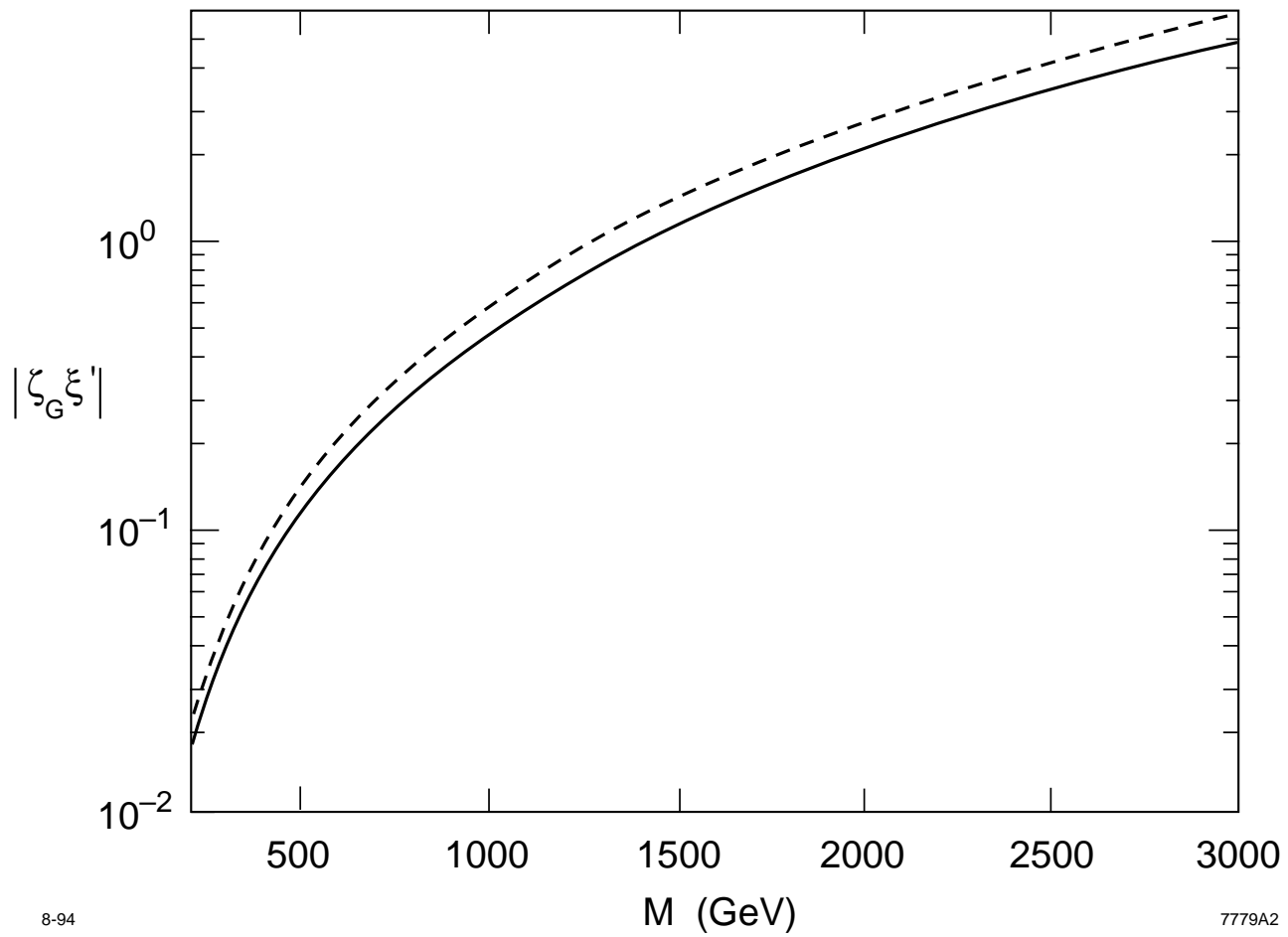


Fig. 1



8-94

7779A2

Fig. 2

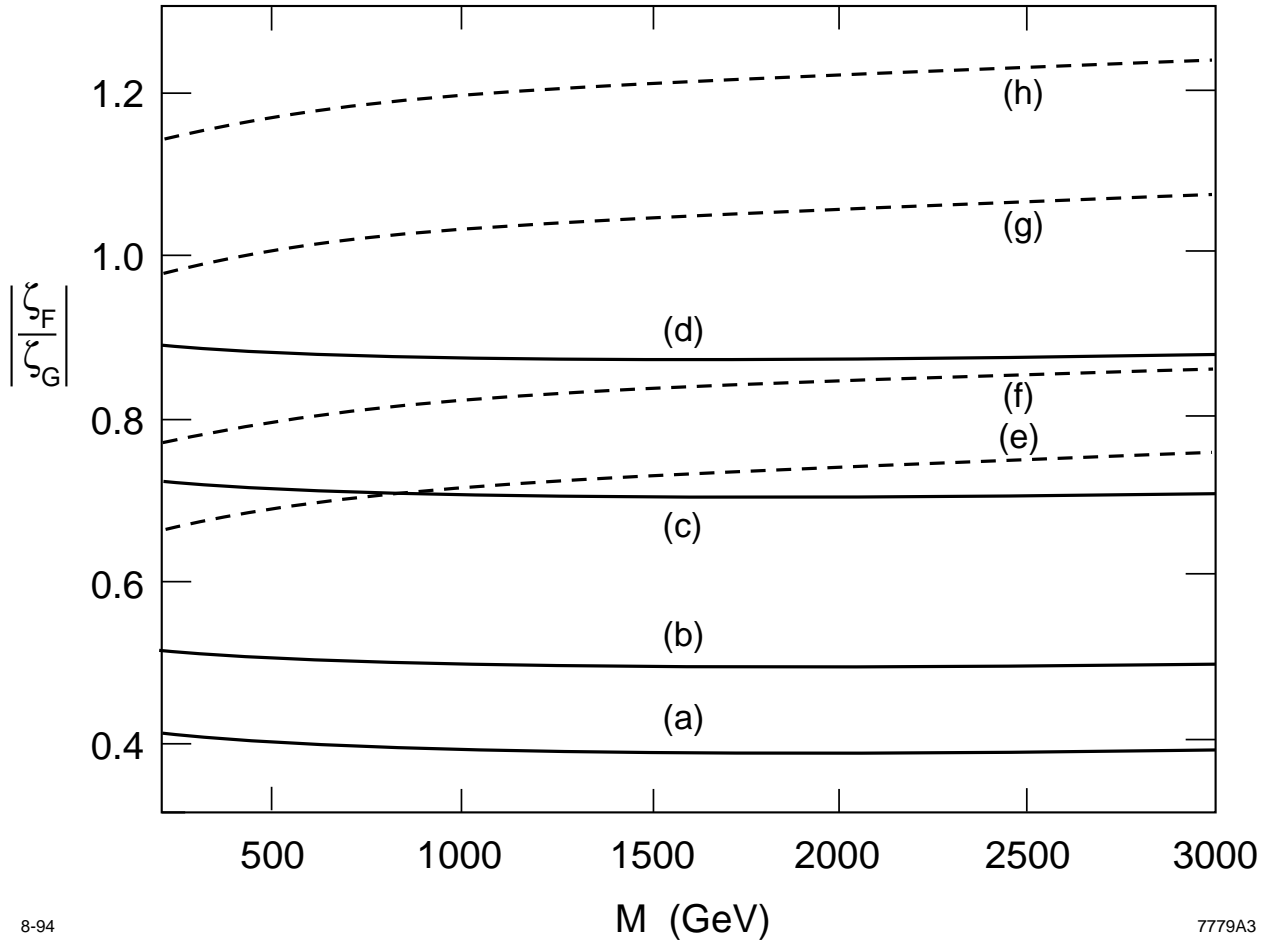


Fig. 3

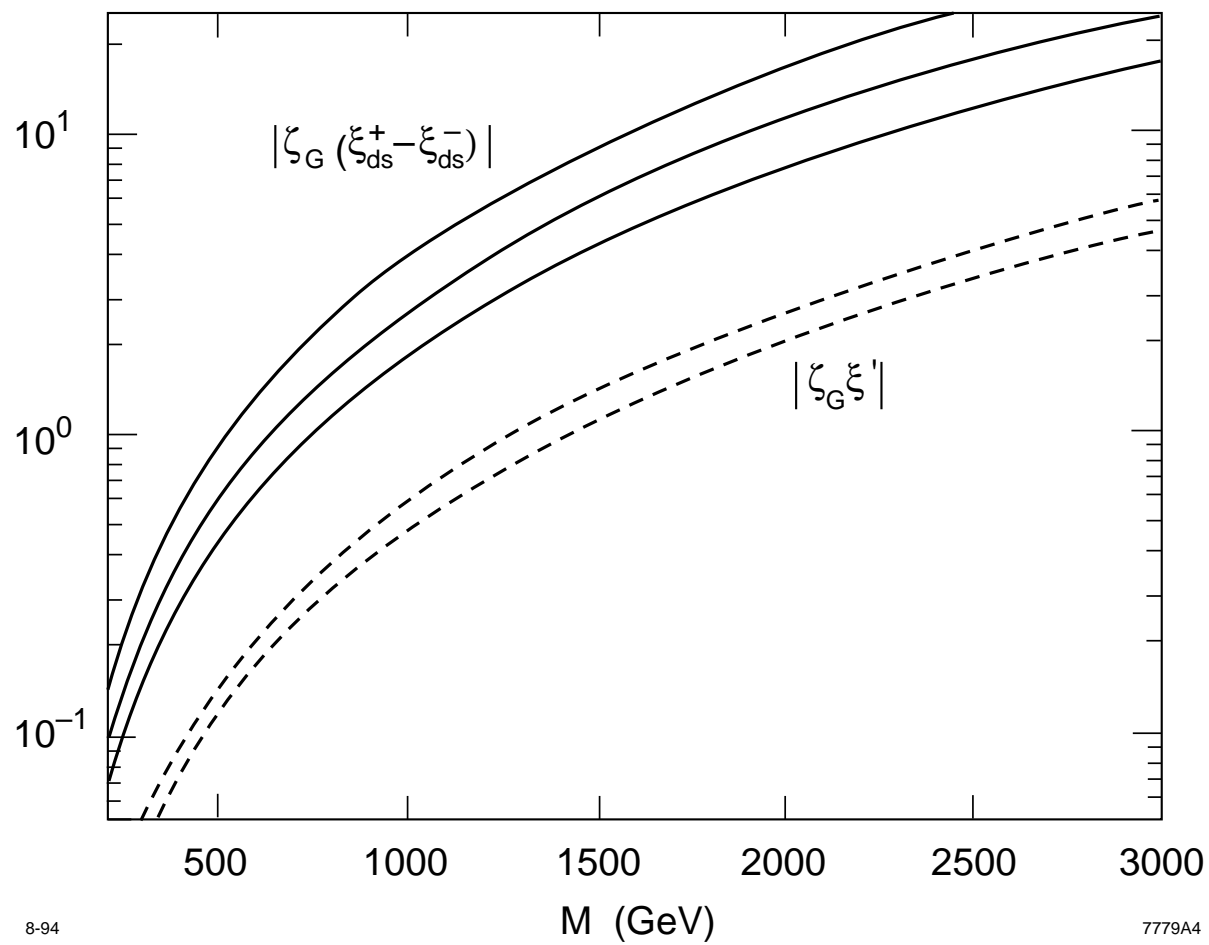
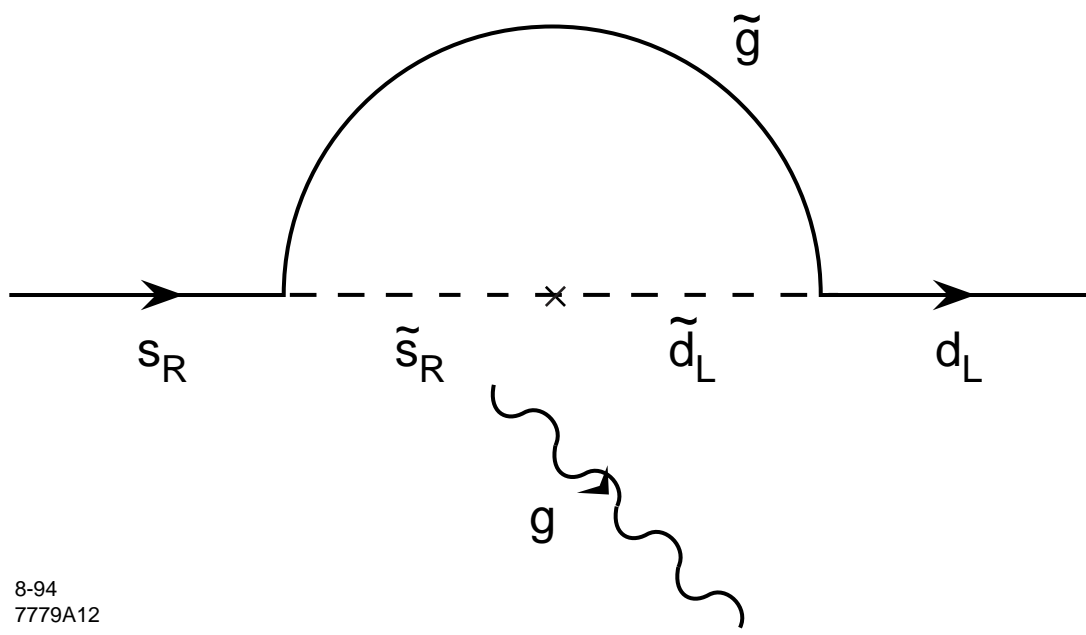


Fig. 4



8-94
7779A12

Fig. 5

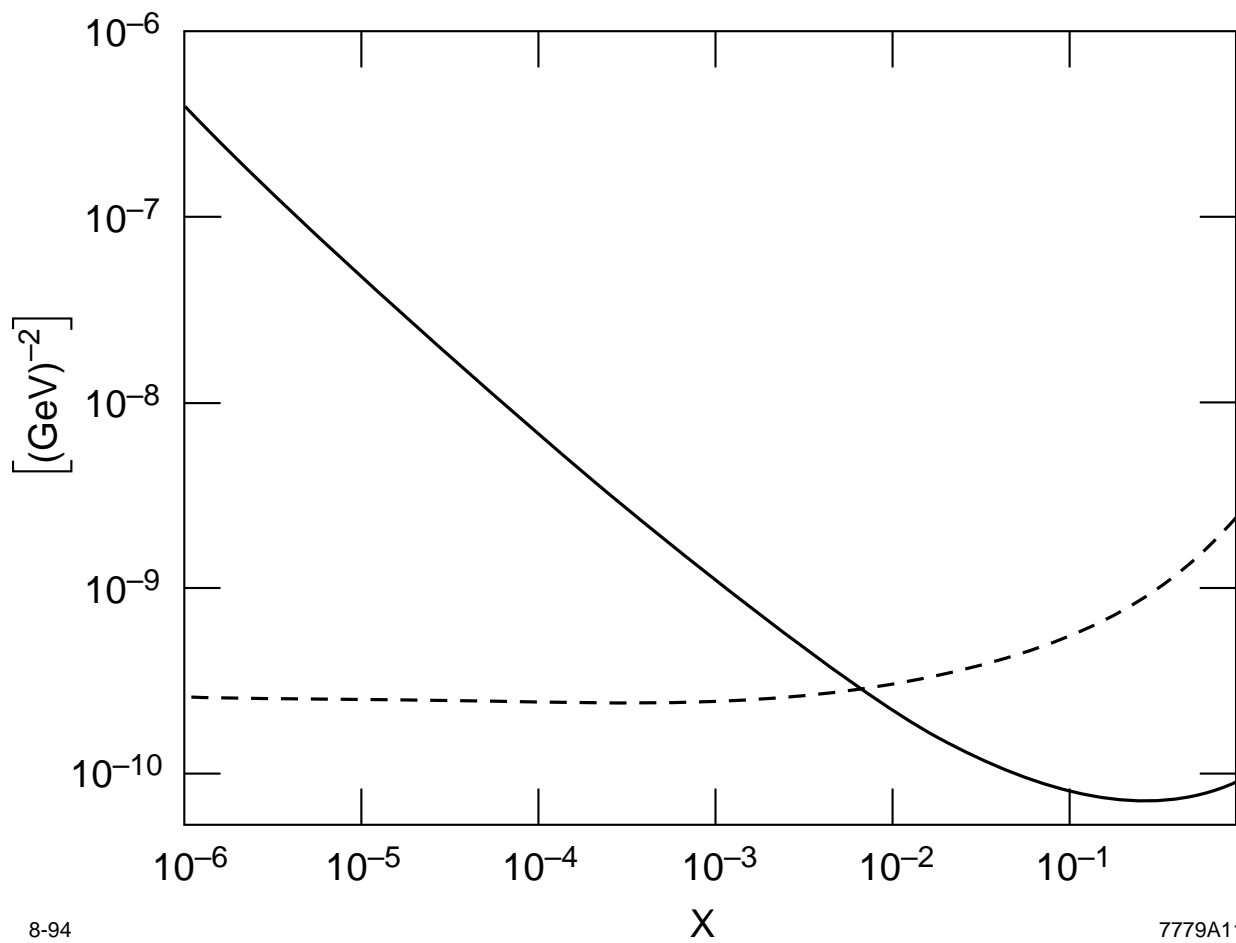


Fig. 6

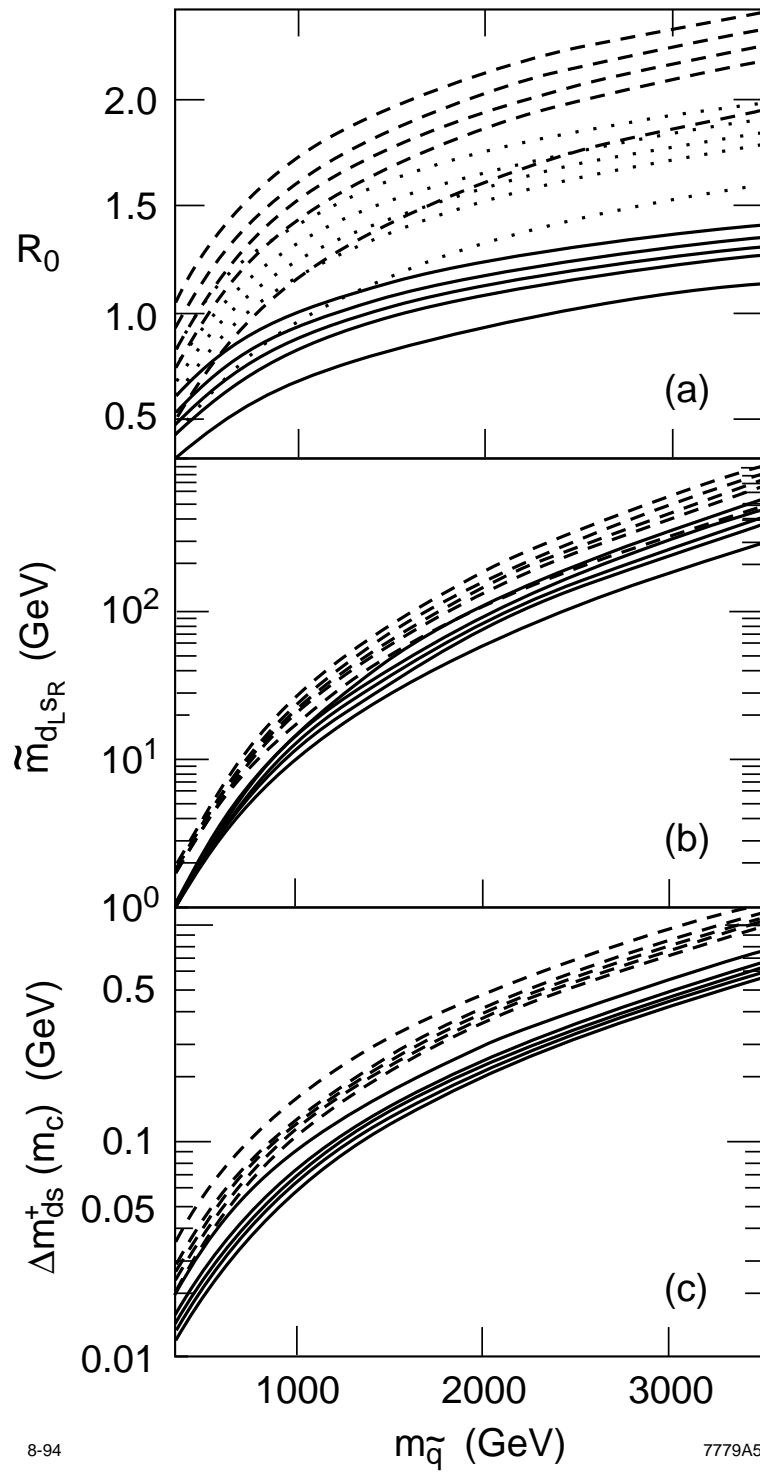


Fig. 7

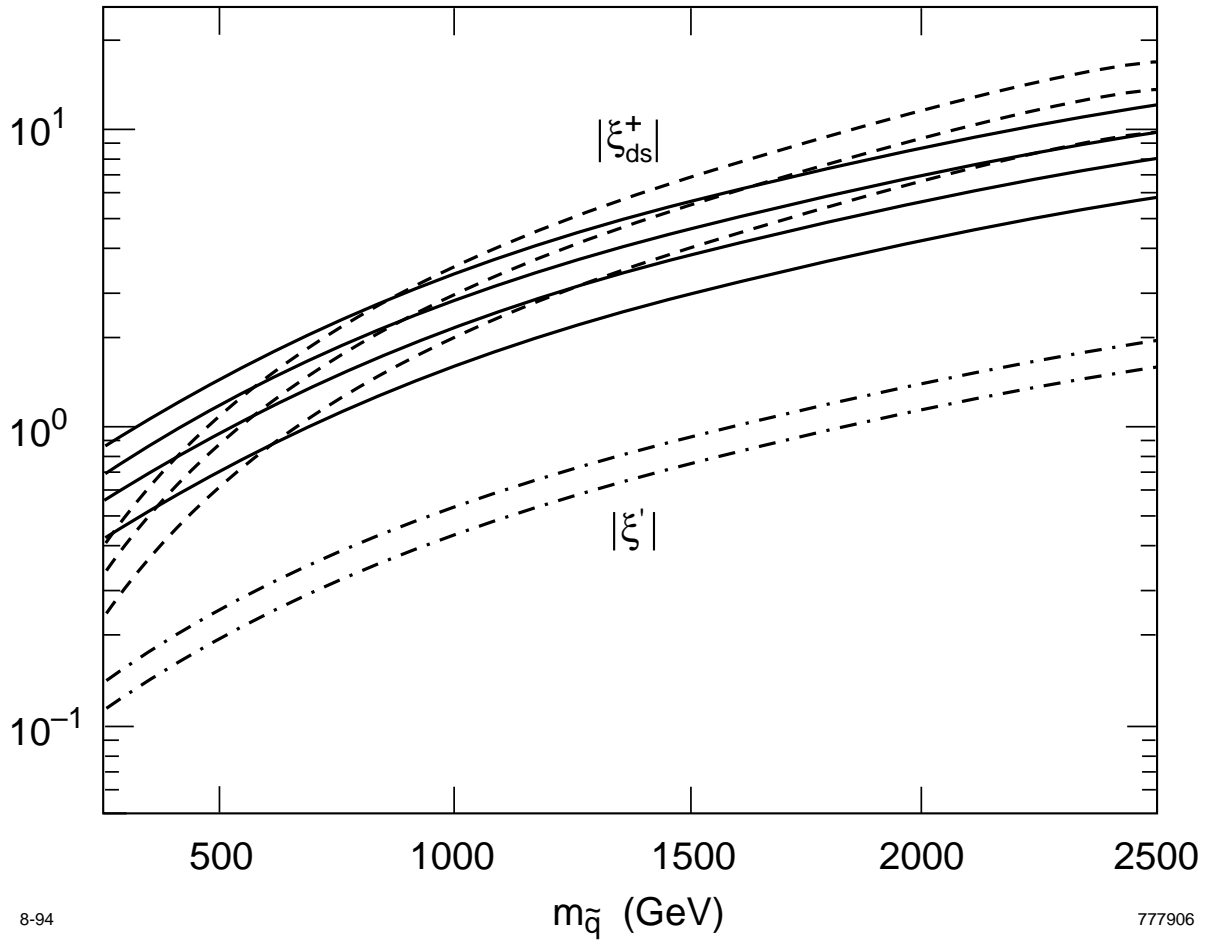


Fig. 8

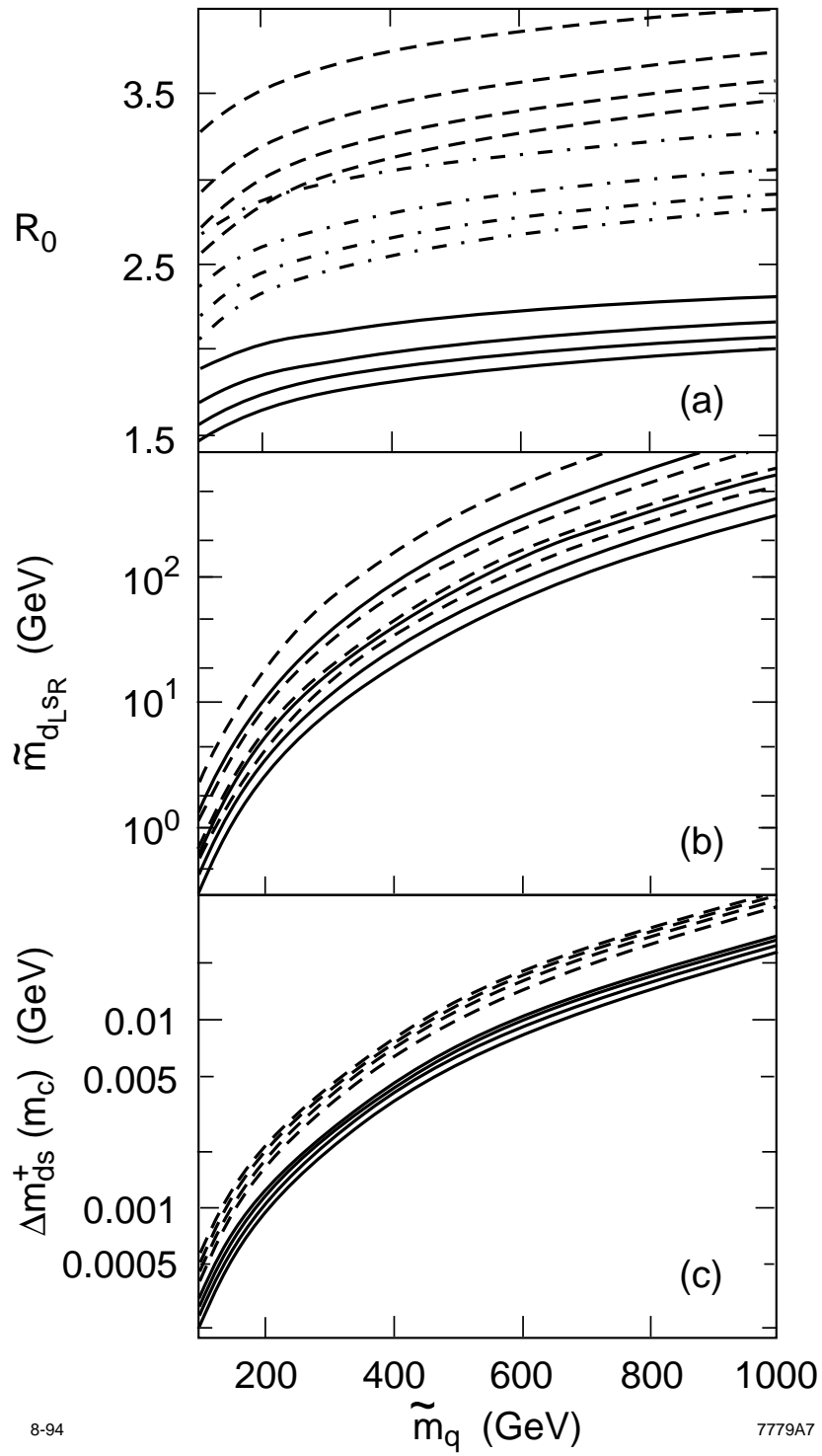


Fig. 9

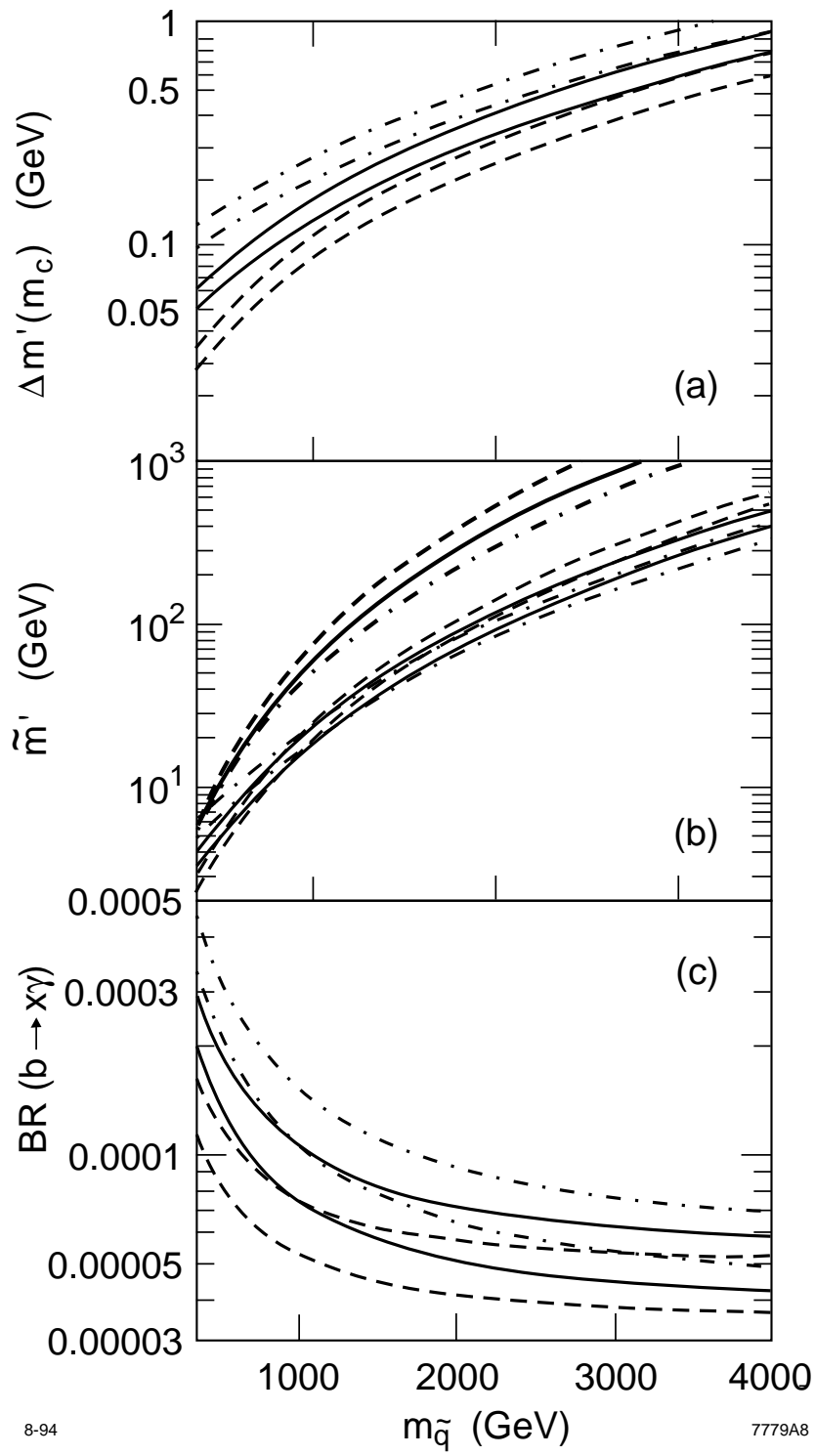


Fig. 10

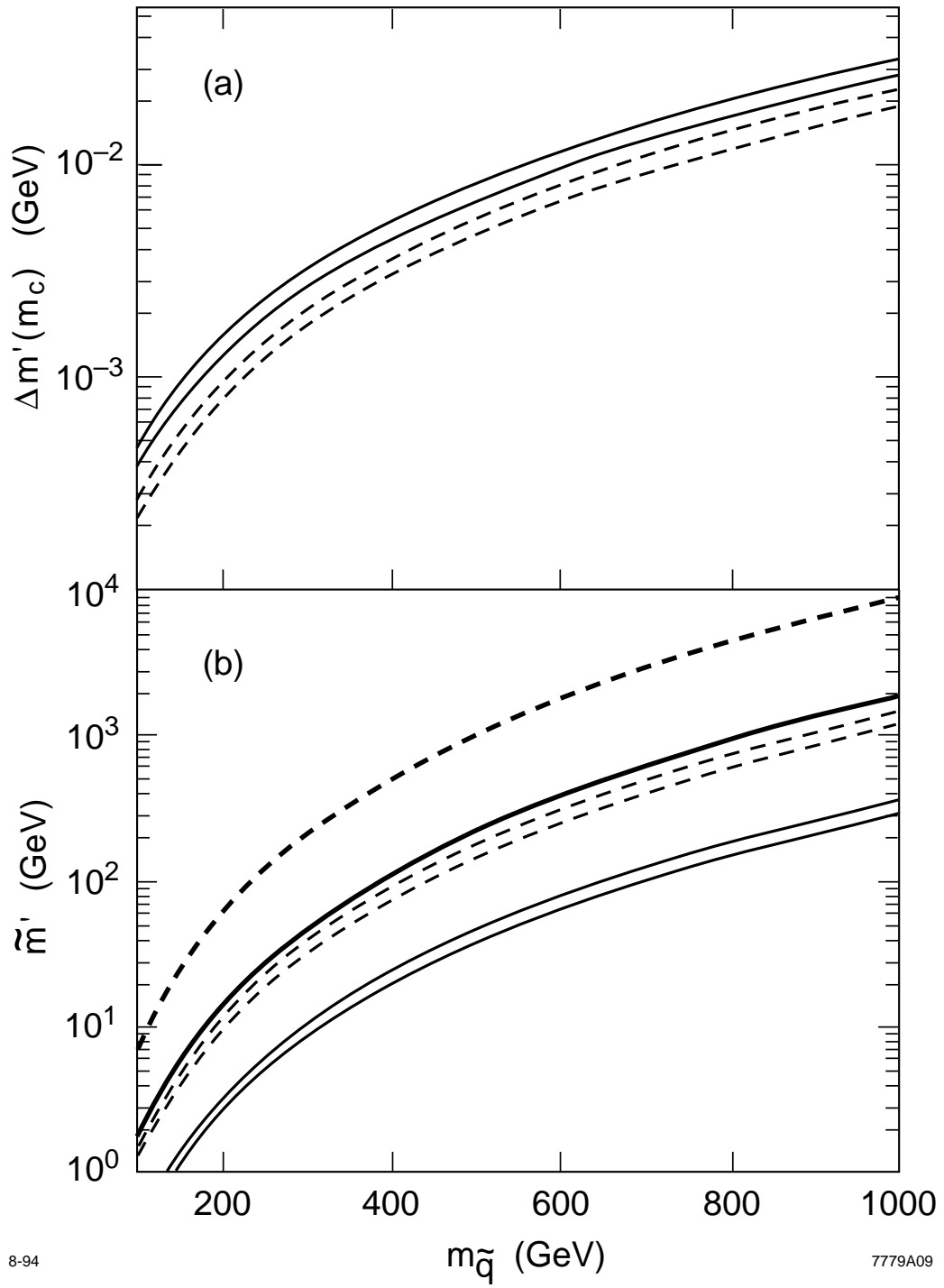


Fig. 11

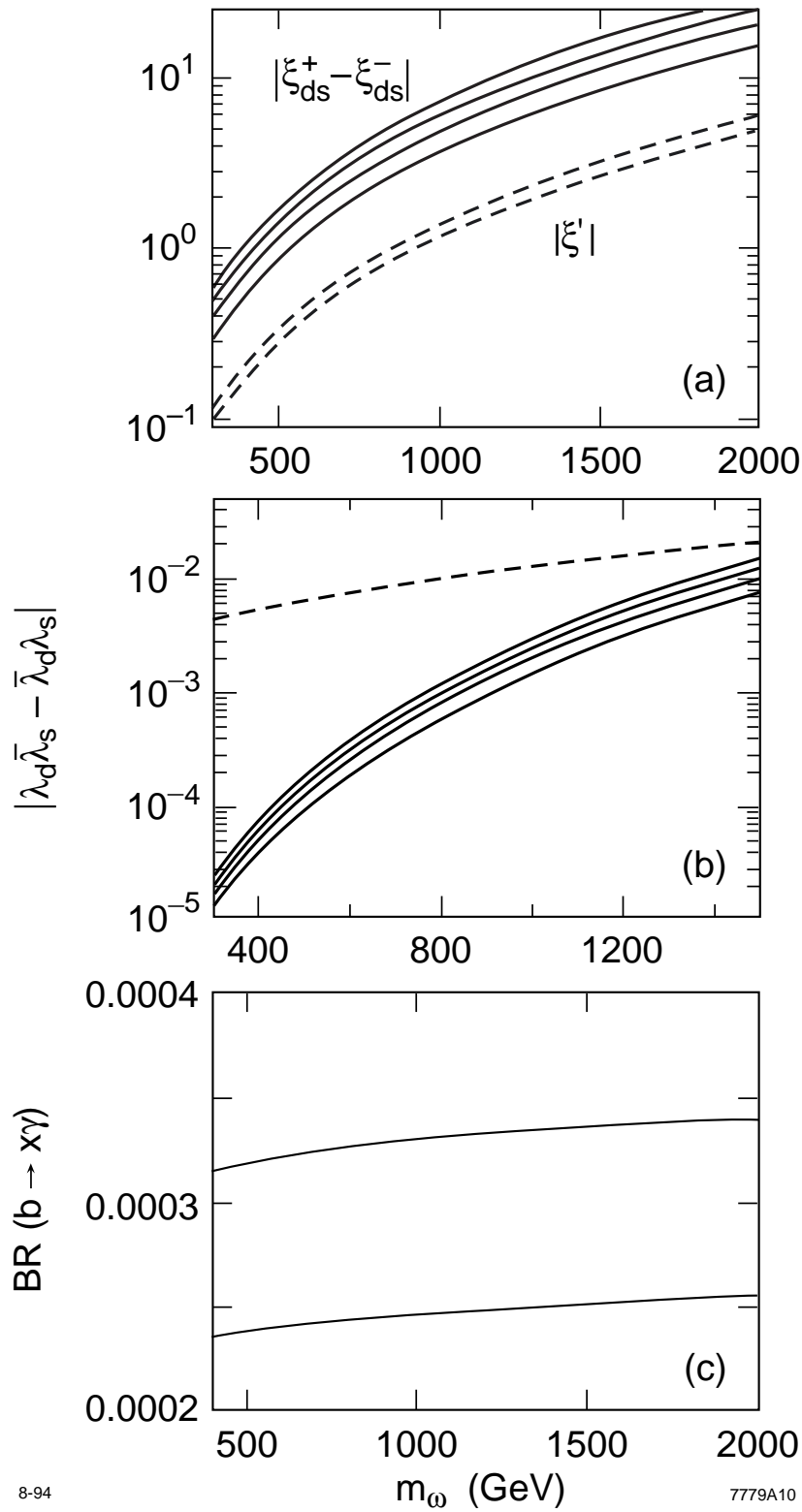


Fig. 12